AD-A056 963 DAVID W TAYLOR NAVAL SHIP RESEARCH AND DEVELOPMENT CE--ETC F/G 13/10
EXPERIMENTAL DETERMINATION OF SCALE, SPEED, AND HULL INTERACTIO--ETC(U)
APR 78 R STAHL

UNCLASSIFIED DTNSRDC/SPD-0396-15 NL

| OF |
AD
A056963

END
DATE
FILMED
9 -78
DDC

DAVID W. TAYLOR NAVAL SHIP
RESEARCH AND DEVELOPMENT CENTER
Bethesda, Md. 20084

EXPERIMENTAL DETERMINATION OF SCALE, SPEED, AND HULL INTERACTION EFFECTS ON HEAVE MOTION COEFFICIENTS OF A SMALL WATERPLANE AREA TWIN HULL SHIP

by

Ralph Stahl

SHIP PERFORMANCE DEPARTMENT
EVALUATION REPORT

March 1973
(Reissued) April 1978

DTNSRDC/SPD-0396-15

MAJOR DTNSRDC ORGANIZATIONAL COMPONENTS

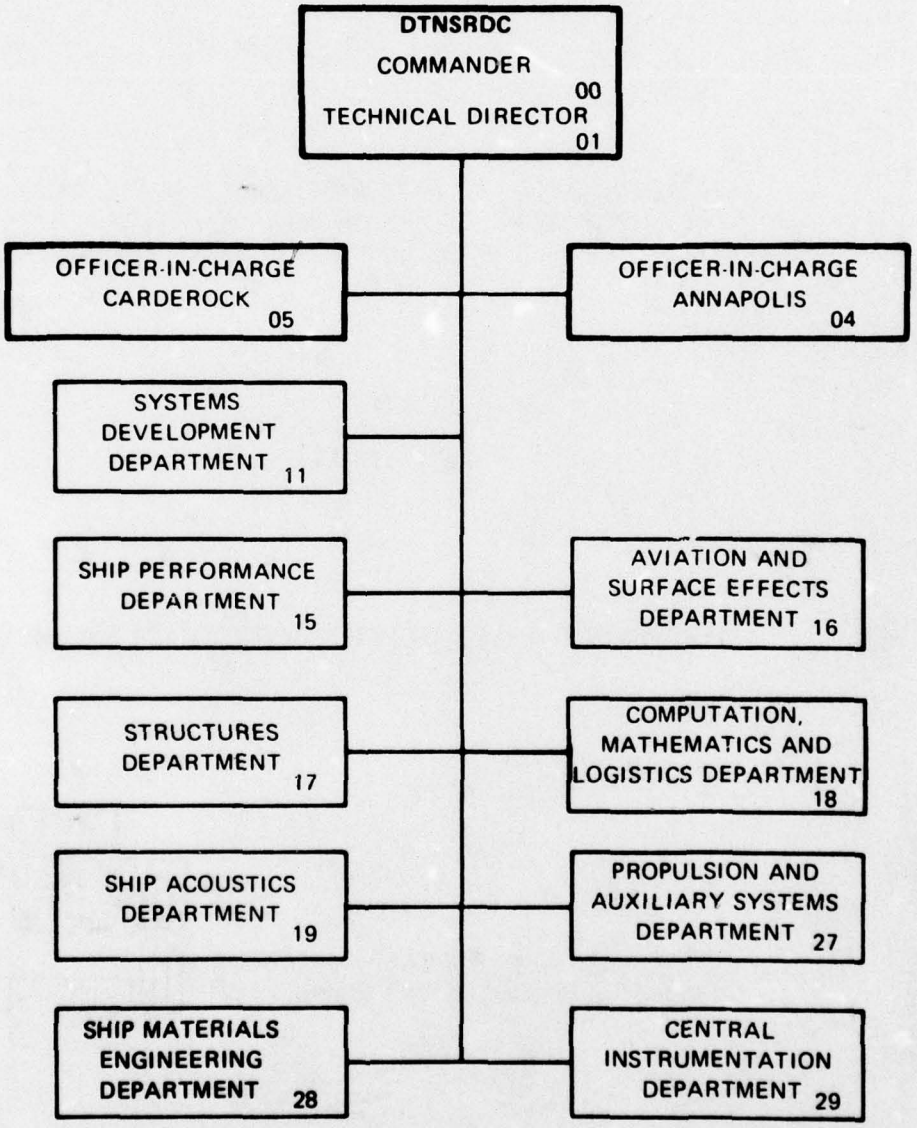

UNCLASSIFIED

SECURITY CLASSIFICATION OF THIS PAGE (When Data Entered)

(14) REPORT DOCUMENTATION PAGE		READ INSTRUCTIONS BEFORE COMPLETING FORM
1. REPORT NUMBER: DTNSRDC/SPD-0396-15	2. GOVT ACCESSION NO.	3. RECIPIENT'S CATALOG NUMBER (9)
(6) 4. TITLE (and Subtitle): EXPERIMENTAL DETERMINATION OF SCALE, SPEED, AND HULL INTERACTION EFFECTS ON HEAVE MOTION COEFFICIENTS OF A SMALL WATERPLANE AREA TWIN HULL SHIP		5. TYPE OF REPORT & PERIOD COVERED: Interim ≠ rept. 3 6. PERFORMING ORG. REPORT NUMBER
7. AUTHOR(s) (10) RALPH STAHL		8. CONTRACT OR GRANT NUMBER(s) (17)
9. PERFORMING ORGANIZATION NAME AND ADDRESS: DAVID W. TAYLOR NAVAL SHIP RESEARCH AND DEVELOPMENT CENTER, BETHESDA, MARYLAND 20084		10. PROGRAM ELEMENT, PROJECT, TASK AREA & WORK UNIT NUMBERS: Element No. 62754 N; Task Area ZF43422001
11. CONTROLLING OFFICE NAME AND ADDRESS: Naval Material Command, Washington, D.C. 20360 (12) 50p.		12. REPORT DATE: March 1973 (Reissued April 1978) (11) 13. NUMBER OF PAGES: 43
14. MONITORING AGENCY NAME & ADDRESS (if different from Controlling Office) (16) F43422		15. SECURITY CLASS. (of this report): Unclassified 15a. DECLASSIFICATION/DOWNGRADING SCHEDULE

16. DISTRIBUTION STATEMENT (of this Report)

Approved for Public Release: Distribution Unlimited

17. DISTRIBUTION STATEMENT (of the abstract entered in Block 20, if different from Report)

18. SUPPLEMENTARY NOTES

19. KEY WORDS (Continue on reverse side if necessary and identify by block number)

Twin Hulls, SWATH, Heave Motion, Hull Interactions, Speed Effects, Size Effects, Experiments

20. ABSTRACT (Continue on reverse side if necessary and identify by block number)

Pure heave oscillation tests were conducted within a range of forward speeds, frequencies, and amplitudes of oscillation on two single hull models representing a small waterplane area design with prime buoyancy derived from the well-submerged bulbous hull. Geometrically, the models differed only in size. Comparing the experimentally obtained non-dimensionalized heave motion coefficients of the two models generally showed independency of model scale, forward speed and especially amplitude of oscillation. The effect of twin-hull interaction on the coefficients

DD FORM 1 JAN 73 1473 EDITION OF 1 NOV 65 IS OBSOLETE S/N 0102-014-6601

389 694

UNCLASSIFIED

SECURITY CLASSIFICATION OF THIS PAGE (When Data Entered)

20
of heave motion was determined with additional experiments on a third model (the twin hulls for the larger model) with the result that interaction was fairly insignificant. The test results with a discussion and conclusion for all three models are presented in this report.

TABLE OF CONTENTS

LIST OF TABLES

LIST OF FIGURES

LIST OF FIGURES (continued)

NOTATIONS

a, b, c, d, e, g	Coefficients in heave equation
D, E, G, A, B, C	Coefficients in pitch equation
A_{33}	Non-dimensional added mass in heave equation
B_{33}	Non-dimensional damping in heave equation
F(t)	Total heave forcing function
F'(t)	Heave forcing function near bow
F"(t)	Heave forcing function near stern
F_s	Force amplitude of in phase component of F(t)
F_s'	Force amplitude of in phase component F'(t)
F_s''	Force amplitude of in phase component F"(t)
F_c	Force amplitude of 90 degree out of phase component of F(t)
F_c'	Force amplitude of 90 degree out of phase component of F' (t)
F_c''	Force amplitude of 90 degree out of phase component of F"(t)
F_n	Froude number $[V/\sqrt{(\text{gravitational acceleration})L}]$
L	Length between perpendiculars (LBP)
M(t)	Pitch forcing function
M_s	Moment amplitude of in phase component of M(t)
M_c	Moment amplitude of 90 degree out of phase component of M(t)

NOTATIONS (continued)

m	Added mass in heave equation
M	Mass of the displaced water
t	Time
T	Total run time
x'	Forward moment arm from LCG to forward block gauge
x''	Aft moment arm from LCG to aft block gauge
$z, \dot{z}, \ddot{z}$	Heave displacement with first and second derivatives in time
$\bar{z}$	Single amplitude in heave oscillation
μ	Non-dimensional frequency of oscillation
γ	Non-dimensionalization of cross-coupling coefficient, D
Φ	Non-dimensionalization of cross-coupling coefficient, $\dot{E}$
$\psi, \dot{\psi}, \ddot{\psi}$	Pitch displacement with first and second derivatives in time
$\bar{\psi}$	Single amplitude in pitch oscillation
ω	Radian frequency of oscillation
α	Phase angle between the applied heave force and heave displacement
β	Phase angle between the applied pitch moment and pitch displacement

ABSTRACT

Pure heave oscillation tests were conducted within a range of forward speeds, frequencies, and amplitudes of oscillation on two single hull models representing a small waterplane area design with prime buoyancy derived from the well submerged bulbous hull. Geometrically, the models differed only in size. Comparing the experimentally obtained non-dimensionalized heave motion coefficients of the two models generally showed independency of model scale, forward speed and especially amplitude of oscillation. The effect of twin hull interaction on the coefficients of heave motion was determined with additional experiments on a third model (the twin hulls of the larger model) with the result that interaction was fairly insignificant. The test results with a discussion and conclusion for all three models are presented in this report.

ADMINISTRATIVE INFORMATION

This work is part of a fundamental study of SWATH type hull forms authorized in Task Area ZF 434-22001, Element No. 62754 N.

INTRODUCTION

In the process of developing analytical prediction methods for the motions of SWATH (Small Waterplane Area Twin Hull) type hull forms in waves, the Naval Ship Research and Development Center is developing a theory for determining the dynamic coefficients of the equations of motion in the heave mode. Experimental verification of the prediction methods for the small waterplane area hull form is important, especially since nonlinear effects in damping and possibly added mass can be present which are not incorporated in present theory. For this purpose two models, differing only in size, were oscillated sinusoidally in heave at various amplitudes and frequencies while the model was towed at several forward speeds. Each model consisted of only a single hull of SWATH I design. Of further interest was the degree to which the two hulls of a SWATH type ship affected each other. Hence, a twin-hulled model was oscillated in the same manner as that used in the single hull oscillation work. The forces and moments needed to impose the vertical displacements for all three models were measured and the results used to compute the coefficients of the heave equations. The coefficients presented here in non-dimensional form were compared to determine the effects of model scale, forward speed, amplitude of oscillation, frequency of oscillation, and hull interaction on heave motion.

MODEL PARTICULARS

The three models used in the pure heave oscillation tests were all of SWATH I design. With reference to Table 1, the first model was a single, small hull with a surface piercing strut. The second and third models were respectively a large, single hull and large twin hulls (Model 5226) both scaled 2.25:1 with respect to the first model. Each hull was completely submerged with only a faired cylindrical strut extending vertically upward piercing the free water surface as shown in Figure 1. Consequently, the strut had a constant waterplane geometry and area with vertical displacement. Geometrically also the strut was symmetrical about both the amidship and the centerline planes.. The hull was a body of revolution about a horizontal axis lying in the centerline plane. The body was nearly symmetrical about amidship except for the stern where design allowances for the propeller were made. Table 1 and Figure 1 give further essential dimensions including the $\mathbb{C}$ to $\mathbb{C}$ twin hull separation of 3.37 feet. The separation of the twin hulls was accomplished by two aluminum channels equally spaced from amidship. For the tests all three models were rudderless, had dummy propeller hubs replacing the stock propellers, and had no turbulance inducing sand strips at the bow. The models were ballasted for zero trim.

EXPERIMENTAL SET UP AND TEST PROCEDURE

Each of the three models was forced to heave sinusoidally about the design waterline (DWL). The oscillator utilized for the tests was the MARK II on Carriage 2 of the Center's Deep Water Basin. Incorporating the SCOTCH Yoke in its design made it possible to achieve very good harmonic heave displacements in the desired frequency range of 0.35 to 3.0 cps. The frequency of oscillation was adjustable by the voltage input to the oscillator's motor.

The block gauge location and the frame used for attaching the single hull and twin hulls to the oscillator are shown schematically as top views in Figure 2. For the small single hull, two $\pm$ 25 pound, 2 inch block gauges were mounted equidistant from amidship and secured to the oscillator by means of a 1 inch thick aluminum plate. The large single hull was similarily mounted using two $\pm$ 500 pound, 4 inch block gauges and an "I" beam structurally connecting the gauges to the oscillator. The same frame with the two $\pm$ 500 pound block gauges was used to attach the twin hulls to the oscillator. In this case, of course, the gauges were mounted onto the two aluminum channels connecting the twin hulls.

In determining scale and speed effects on the heave motion coefficients for the small and large single hulls of SWATH I, Froude scaling was used. The selected speeds in equal increments were F_n = 0, 0.20, 0.40, and 0.60, which corresponded to 0, 1.47, 2.93, and 4.40 knots for the small model and 0, 2.20, 4.40, and 6.60 knots for the large model. Single amplitudes of oscillation were 0.17 , 0.22, 0.63, and 1.20 inches for the small model, 0.38, 0.50, 1.40, and 2.70 inches for the large single hull and 1.40, 2.00, and 2.70 inches for the large twin hull configuration. For each of the

speeds and amplitudes, the heave oscillation was within 0.53 and 3.00 cycles per second for the small model and 0.35 to 2.00 cps for the large models with the exception of the twin hull configuration where higher frequencies had to be deleted due to excessive forces.

Concurrent to oscillating the twin hulls in heave, an attempt was made to determine the height of the craft generated waves between the two hulls by placing an ultrasonic transducer at various stations midway between the hulls. However, because a standing wave pattern existed for all investigated speeds, frequencies, and amplitudes, frequent signal "drop out" occurred. This occurred whenever the wave slope was significantly large in the area of the transducer. This problem could have been alleviated by using a horizontal array of transducers; however, considering the difficulties encountered with the ultra sonic probe together with possible interference effects between them an alternative transducer should be used as for example the electrical resistivity of vertically stretched wires in a horizontal array. Since this method was beyond the intended scope of the experiments and since the data obtained with the single ultrasonic probe was meaningless, no quantitative twin hull generated wave results are presented in this report.

with the in and 90 degrees out of phase heave force components F_s and F_c given by the expressions

$$F_s = F_s' + F_s'' \tag{10}$$

$$F_c = F_c' + F_c'' \tag{11}$$

Inserting z and its derivatives into expression (3), and equating the coefficients with like terms gives the following two parameters:

$$a = \frac{\bar{z}\, c - F_s}{\bar{z}\omega^2} \tag{12}$$

$$b = \frac{F_c}{\bar{z}\omega} \tag{13}$$

Experimentally obtaining c is achieved by vertically displacing the model and measuring the resultant force. Computationally, the weight of the displaced water for a given vertical displacement must be determined from the geometry of the model. The restoring coefficient for each of the three models tested are presented in Table 1 and are used in all subsequent calculations. The coefficient was a constant for each model since only the cylindrical strut, which had a constant waterplane area, ever pierced the free water surface.

The cross-coupling coefficients D and E can be obtained in a manner very similar to that already used for obtaining the dynamic coefficients of the force equation. The moment function, M(t), in its basic components can be written as:

$$M(t) = M_s \sin(\omega t) + M_c \cos(\omega t) \tag{14}$$

For the harmonic oscillation tests conducted in pure heave only, equations (1) and (2) can be simplified. Since pitching motion is totally absent, ψ and its derivatives $\dot{\psi}$ and $\ddot{\psi}$ are all equal to zero. Equations (1) and (2) then become respectively

$$a\ddot{z} + b\dot{z} + cz = F(t) \tag{3}$$

$$D\ddot{z} + E\dot{z} + Gz = M(t) \tag{4}$$

Obtaining the acceleration and velocity coefficients in force equation (3), the function must first be reduced to its basic components, i.e.:

$$F(t) = F_s \sin(\omega t) + F_c \cos(\omega t) \tag{5}$$

where the term $F_s \sin(\omega t)$ is in phase and $F_c \cos(\omega t)$ is 90 degrees out of phase with the heave motion. For a nearly harmonic forcing function of period $\frac{2\pi}{\omega}$, equation (5) is the most significant portion of the Fourier series of F(t), Reference [2]. The forcing function F(t) given here is furthermore the sum of the forward force function F'(t) and the aft force function F"(t). The Euler formulas of the series are:

$$F_s' = \frac{2}{T}\int_o^T F'(t) \sin(\omega t)\, dt \tag{6}$$

$$F_s'' = \frac{2}{T}\int_o^T F''(t) \sin(\omega t)\, dt \tag{7}$$

$$F_c' = \frac{2}{T}\int_o^T F'(t) \cos(\omega t)\, dt \tag{8}$$

$$F_c'' = \frac{2}{T}\int_o^T F''(t) \cos(\omega t)\, dt \tag{9}$$

The force signal in analog form of the forward block gauge, $F'(t)$, and the aft block gauge, $F''(t)$, were used to electronically obtain F_s', F_s'', F_c' and F_c''. Each of the two signals was multiplied by sin (ωt) and cos (ωt) utilizing two sine and two cosine potentiometers respectively. The potentiometers were linked mechanically to the oscillator in order to rotate at the frequency of oscillation and in phase with the oscillation. The products $F'(t)$ sin (ωt), $F''(t)$ sin (ωt), $F'(t)$ cos (ωt), and $F''(t)$ cos (ωt) were then integrated over an integral number of cycles ranging from 1 to 10 cycles of oscillation. Multiplying each of the four integrated values by 2/T gave F_s', F_s'', F_c', and F_c''. These force amplitudes were substituted into equations (10) thru (13) together with the known values of $\bar{z}$ and c to get a and b. Similarly a substitution into equations (15) thru (18) with the known values of $\bar{z}$, C, and ω allowed equations (15) and (16) to be solved for D and E.

DISCUSSION OF RESULTS

All of the experimentally determined dynamic coefficients presented here are non-dimensionalized by the techniques used in previous harmonic oscillation tests with a catamaran, ~~see Reference~~ [1], and the techniques indicated by Program YF17, see Reference [2]. The static restoring coefficients, c, for the three models are constants within the heave amplitudes investigated and are presented in Table 1. The cross-coupling coefficient, G, is zero as stated earlier. Before non-dimensionalizing the previously calculated dynamic coefficients of the force equation, a must first be expressed in terms of its two components, i.e.

$$a = M + m \tag{19}$$

where M = mass of the displaced water

m = added mass

The added mass, m, damping coefficient, b, and the frequency of heave oscillation μ, become in non-dimensionalized form:

$$A_{33} = \frac{m}{M} \tag{20}$$

$$B_{33} = \frac{b}{M\sqrt{\text{gravitational acceleration}/L}} \tag{21}$$

$$\mu = \omega\sqrt{L/\text{gravitational acceleration}} \tag{22}$$

where L = length between perpendiculars (LBP)

Non-dimensionalizing the dynamic cross-coupling coefficients, D and E, of the moment equation, the following results were obtained

$$A_{53} = -\frac{D}{ML}$$

$$B_{53} = \frac{-E}{ML\sqrt{\text{gravitational acceleration}/L}}$$

The non-dimensionalized added mass and the non-dimensionalized damping versus non-dimensionalized frequency are presented in Figures 3a thru 8d with first the small, single hull model followed by the large, single hull model and finally the large, twin hulls. The figure subgrouping a, b, c, and d are for the four speeds F_n = 0, 0.20, 0.40, and 0.60 respectively. In general, the added mass and damping for all three models indicated good repeatability. The non-dimensionalized coefficients A_{53} and B_{53} were found to be very small in magnitude. This was anticipated

since all three models were nearly symmetrical about midship. Due to the insignificance of the results for the two cross-coupling coefficients, they are not presented in this report.

In discussing the effects of amplitude of oscillation, model speed, and scaling on the added mass and damping of a single hull of SWATH I, reference is made to Figures 3a thru 6d. Except for a few isolated incidents, both added mass and damping were markedly linear with oscillation amplitude in the investigated non-dimensionalized frequency range of 1.2 to 7.4 and the speed range of F_n = 0 to 0.6 for both models. The exceptions were primarily at the very lowest frequencies where inaccuracies in measurement can be expected, ~~see Reference 4~~. Both dynamic coefficients A_{33} and B_{33}, were also generally independent of forward model speed. The added mass for the small model in Figures 3a thru 3d showed a common trend of being inversely proportional to frequency up to about μ = 2.7, whereafter A_{33} increased with frequency almost asymptotically to an approximate value of A_{33} = 0.43. With increasing model speed, the slope decreased slightly for frequencies greater than μ = 2.7. Damping for the same model, given in Figures 4a thru 4d, showed some dependency on speed in the low frequency range up to μ = 2.7. Here the damping coefficient B_{33} increased with increasing model speed particularly for Froude numbers greater than 0.2. For frequencies greater than μ = 2.7, damping became both independent of model speed and linear with frequency. The added mass for the large, single hull SWATH I (Figures 5a thru 5d) was almost

identical to the results obtained for the small model with the exception that the dip in A_{33} at the frequency of $\mu = 2.7$ was almost not noticeable and the asmptotic value of $A_{33} = 0.43$ was approached much faster with increasing frequencies. The damping coefficients (Figures 6a thru 6d) showed trends similar to those encountered with the small model except for a reduction in magnitudes especially for higher frequencies and a negligible speed dependency. Comparing the non-dimensionalized added mass of the two models differing only in size thus showed general independence to model scale whereas the non-dimensionalized damping indicated some scale dependency primarily in the high frequency range.

Hull interaction effect on added mass and damping is discussed with reference to Figures 5a thru 6d for the large single hull and Figures 7a thru 8d for the large twin hulls. The added mass for the large single hull, as discussed earlier (see Figures 5a thru 5d), was generally inversely proportional to frequency up to approximately $\mu = 2.7$ where a constant value of $A_{33} = 0.43$ was reached. Linearity with amplitude of oscillation and speed independency was especially good for frequencies greater than $\mu = 3$. Damping for the same model (see Figures 6a thru 6d) was speed independent and linear with amplitude. The twin hulls, having $\mathcal{L}$ to $\mathcal{L}$ hull separation of 3.37 feet, has values for A_{33} that differed somewhat from the single hull case in both magnitude and trend. With reference to Figures 7a thru 7d, the slope of A_{33} for low frequencies gradually became more positive with increasing model speed as opposed to the consistently negative slope for the single hull. With increasing frequency, A_{33} approached a constant value of about $A_{33} = 0.50$ as compared to the single hull case of $A_{33} = 0.43$.

Damping characteristics for the twin hull model shown in Figures 8a thru 8d, were similar to the trends for the single hull. In both cases damping generally decreased up to a frequency of $\mu = 2.7$ and increased linearily with frequency. Hull interaction was thus found to affect the non-dimensionalized added mass, especially for higher model speeds whereas non-dimensionalized damping was not notably affected.

CONCLUSIONS

Based on the results of harmonically oscillating two single hulls differing in size and one twin hull configuration all of SWATH I design, the following conclusions are made concerning the effects of model scale, forward speed, amplitude of oscillation, and hull interaction on the dynamic coefficients of the heave equation:

1. Model Scaling - Froude scaling is applicable within the limits of the investigated single hull model sizes and frequency range for added mass. For damping, Froude scaling is applicable primarily in the low frequency range.

2. Forward Model Speed - Added mass and damping are generally independent of forward speed for the three models. Notable exceptions are:

   a. For the small single hull the dip in added mass at $\mu = 2.7$ disappeared with increasing speed. Damping also increased with speed at the very lowest frequency of $\mu = 1.2$.

b. For the large twin hulls added mass decreased with speed at the low frequency range of $\mu = 1.2$ to about 2.

3. Force Linearity with Amplitude - Force linearity with amplitude of oscillation is clearly present in all instances within the speed and frequency ranges tested of both single hulls and twin hulls.

4. Hull Interaction - No noticeable hull interaction on damping is evident but the affect on added mass is a decrease in the low frequency range for higher model speeds and an approximate 16 percent increase for frequencies greater than $\mu = 2$.

ACKNOWLEDGMENTS

The author wishes to express his appreciation to Messrs. M. Davis, J. Bonilla-Norat, and R. Duerr who participated in the test program.

REFERENCES

1. Jones, Harry D., "Experimental Determination of Coupled Catamaran Pitch and Heave Motion Coefficients," Naval Ship Research and Development Center T & E Report No. 348-H-03, June 1970.

2. Stahl, Ralph G., "Experimental Determination of Heave, Added Mass and Damping of Two-Dimensional Bulbous Cylinders at the Free Water Surface," Naval Ship Research and Development Center T & E Report No. ~~516-H-01~~ 356-17-14, March 1973.

3. Frank, W. and Salvesen, N., "The Frank Close-Fit Ship-Motion Computer Program," Naval Ship Research and Development Center, Department of Hydromechanics Technical Note No. 105, September 1969.

4. Wahab, Rama, "Added Mass and Damping of Bulbous Cylinders Heaving on the Water Surface," Naval Ship Research and Development Center T & E Report No. 227-H-12, March 1970.

TABLE I

MODEL PARTICULARS FOR SMALL WATERPLANE AREA
TWIN HULL SHIP I (SWATH I)

Static and Geometric Characteristics	Small Single Hull	Large Single Hull	Large Twin Hulls
Scale Ratio of Small Model to Large Model	1:2.25		
LBP, ft.	4.77	10.74	10.74
Beam at Midship, ft.	0.19	0.42	3.79
Hull Separation from $\mathcal{L}$ to $\mathcal{L}$			3.37
Vertical distance from baseline to WL, ft.	0.62	1.39	1.39
Waterplane Area, $ft.^2$	0.80	4.05	8.10
LCG aft of F.P., ft.	2.32	5.21	5.21
Water Surface Piercing Cylindrical Struts(s):			
Length, ft.	4.77	10.74	10.74
Beam, ft.	0.19	0.42	0.42
Circular Submerged Hull(s):			
Overall length from bow to end of propeller hub, ft.	5.71	12.85	12.85
Diameter at Midship, ft.	0.33	0.75	0.75
Fresh Water Displacement, lbs	42.1	479.1	958.2
Model Weight, lbs	44.7	539	947
Fresh Water Restoring Coefficient in Heave (within the limits of $\pm$ 0.63 ft. from DWL), lbs/ft.	49.9	252.5	505.0

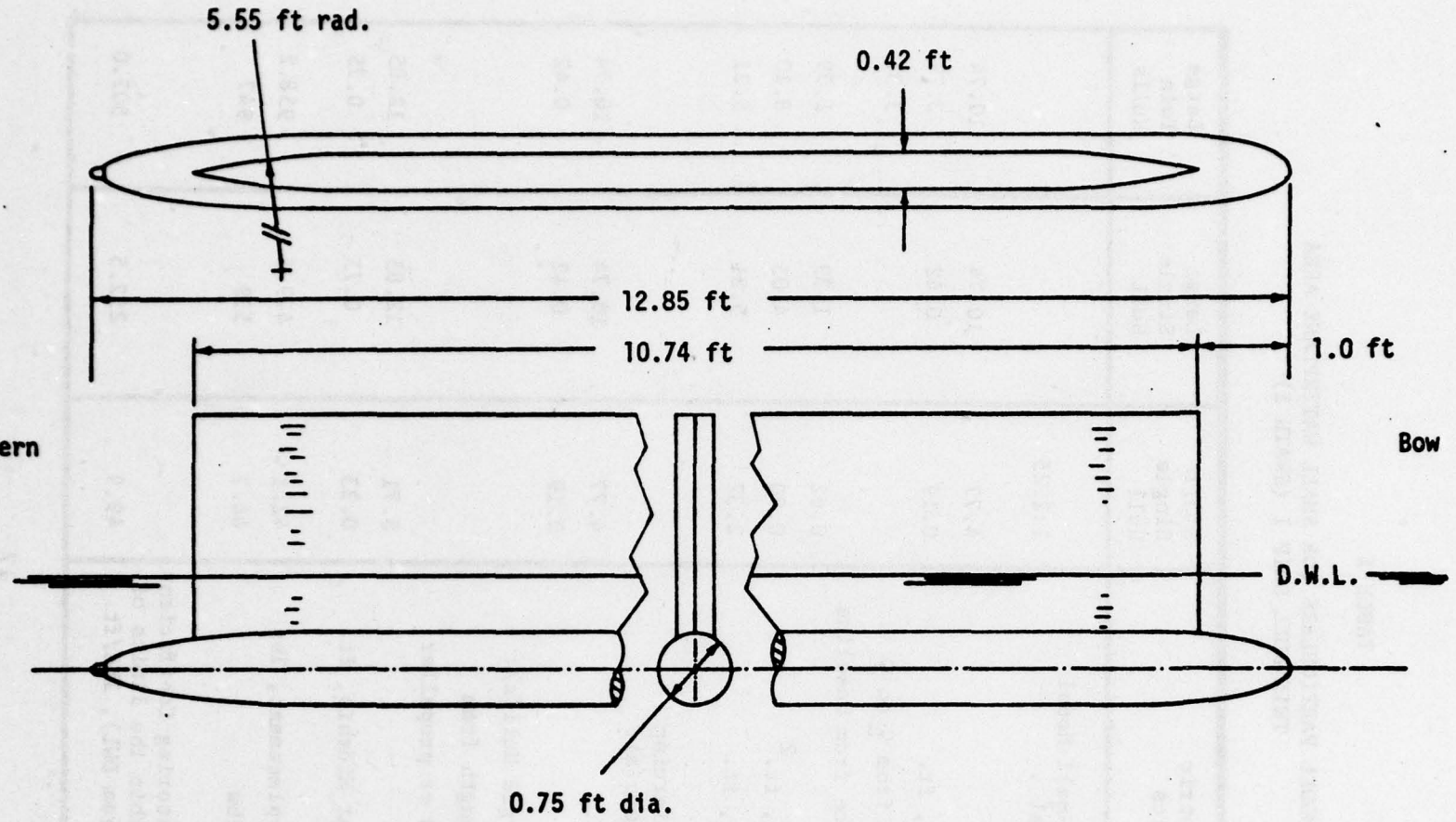

Figure 1 - Sketch of a Single Hull of the SWATH I with the Large Model Dimensions

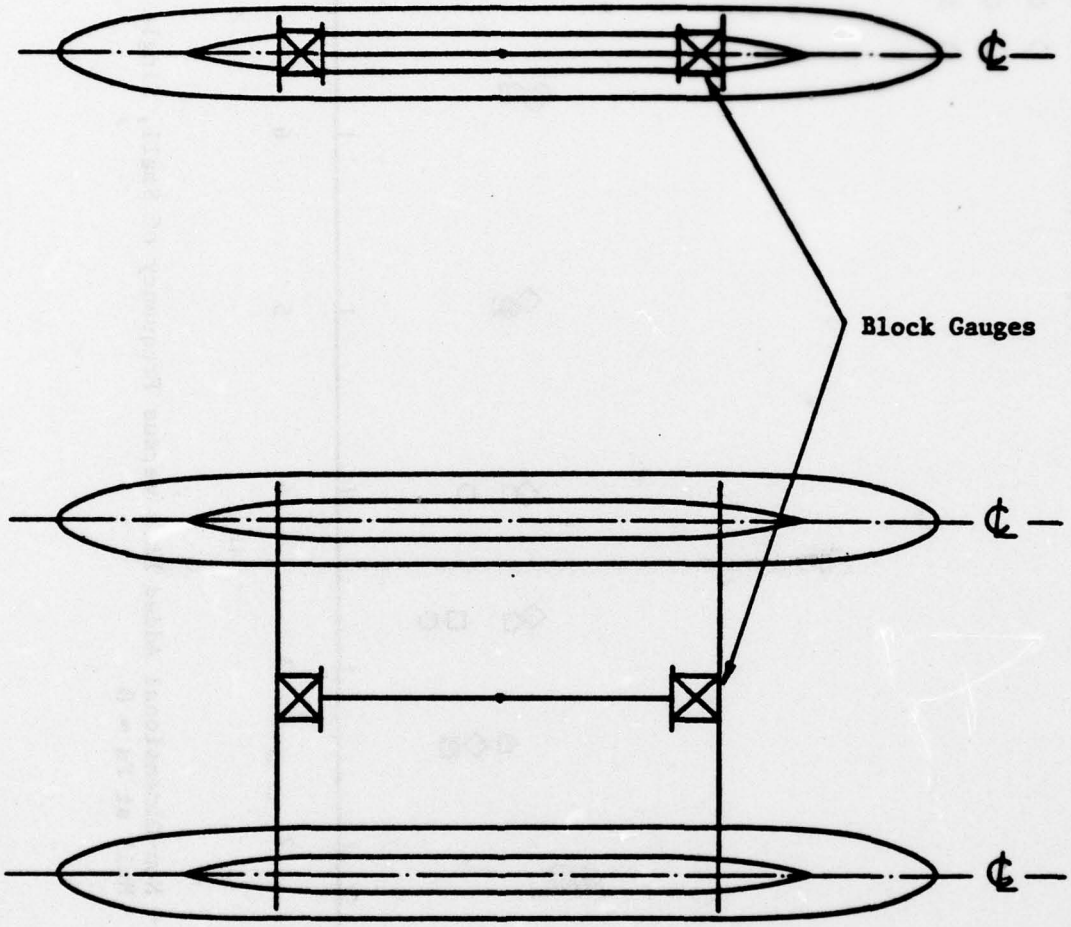

Figure 2 - Test Configuration (Top View) for Oscillating the Single Hull and the Twin Hulls of SWATH I in Heave

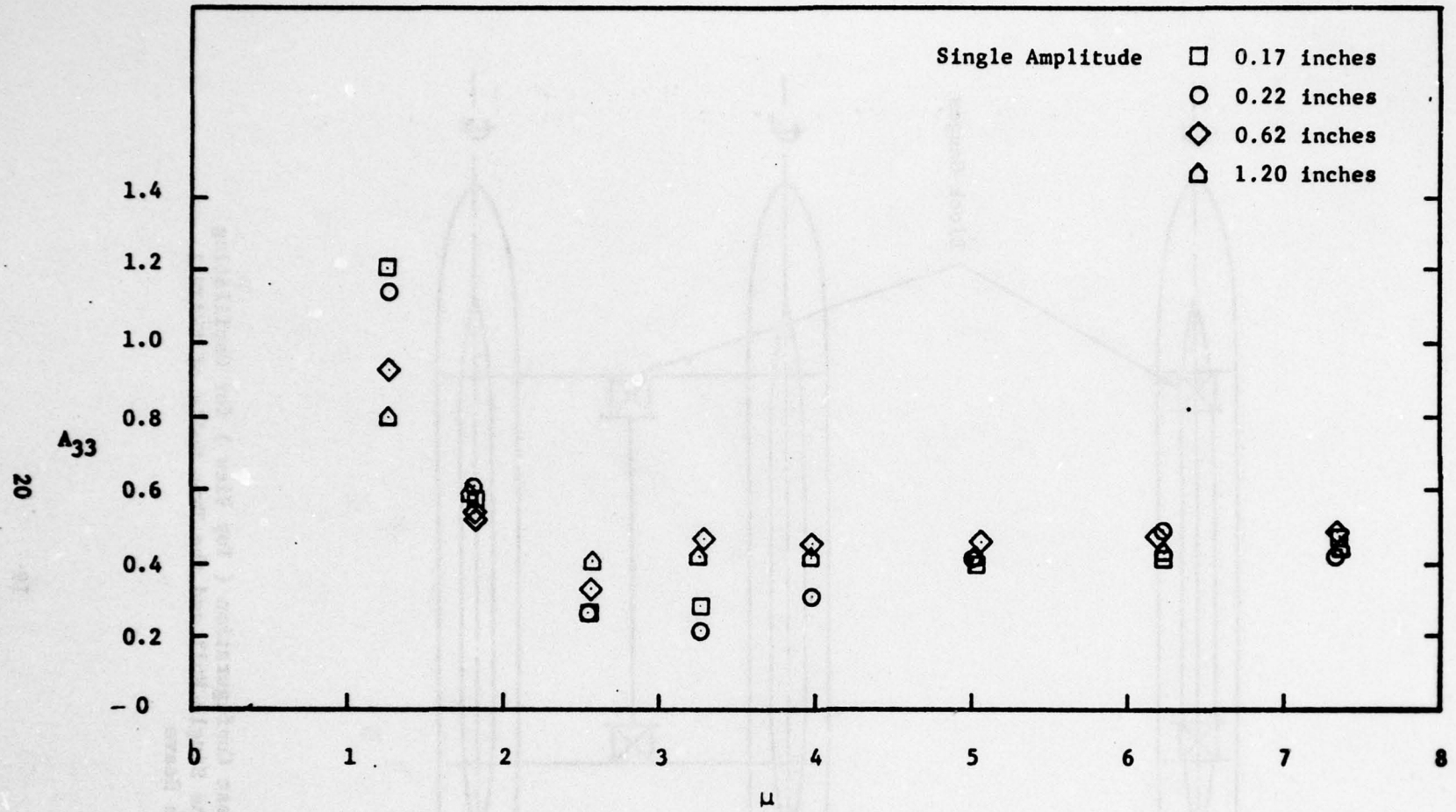

Figure 3a - Non-Dimensional Added Mass versus Frequency of Small, Single Hull at Fn = 0

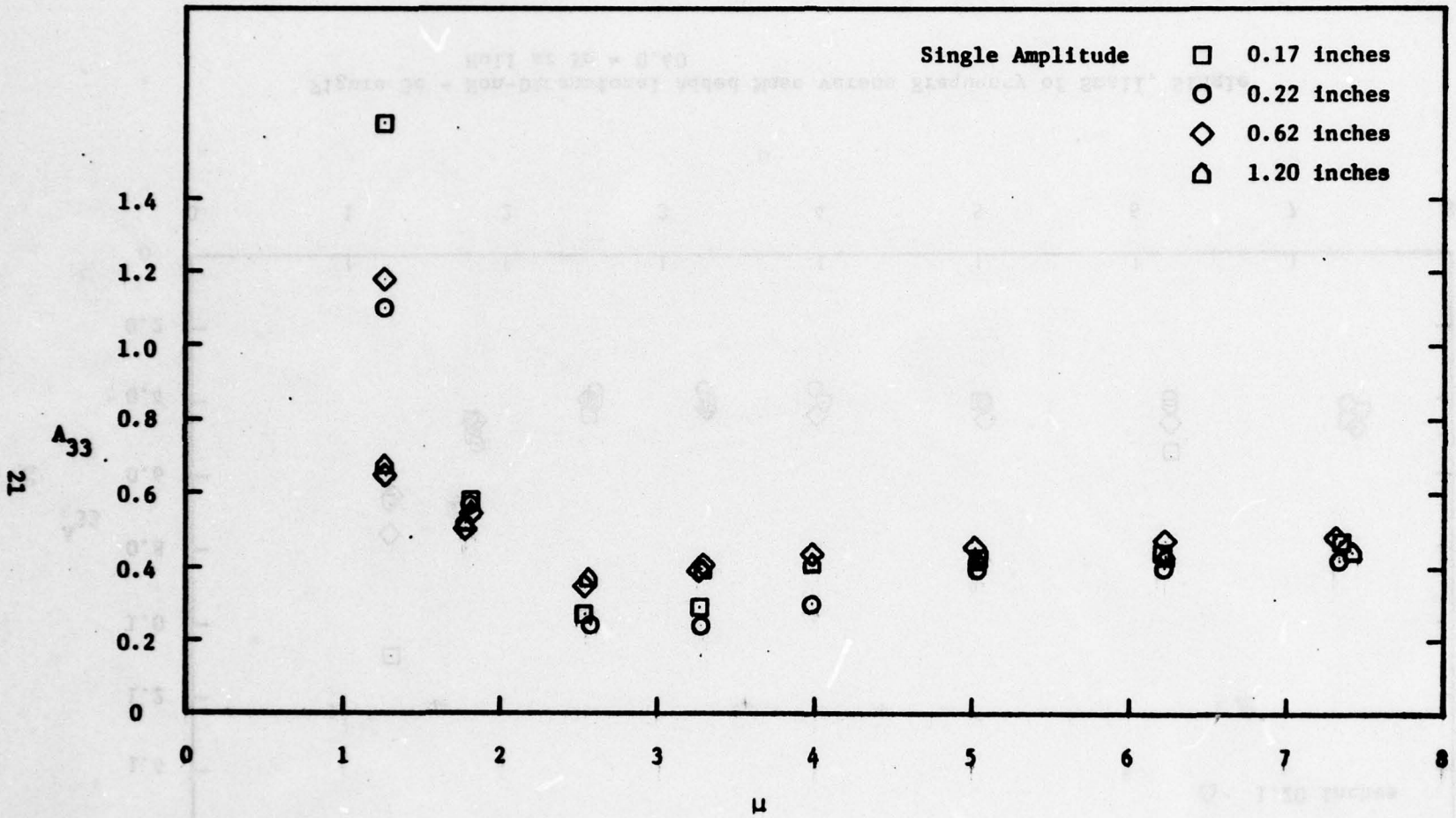

Figure 3b - Non-Dimensional Added Mass versus Frequency of Small, Single Hull at Fn = 0.20

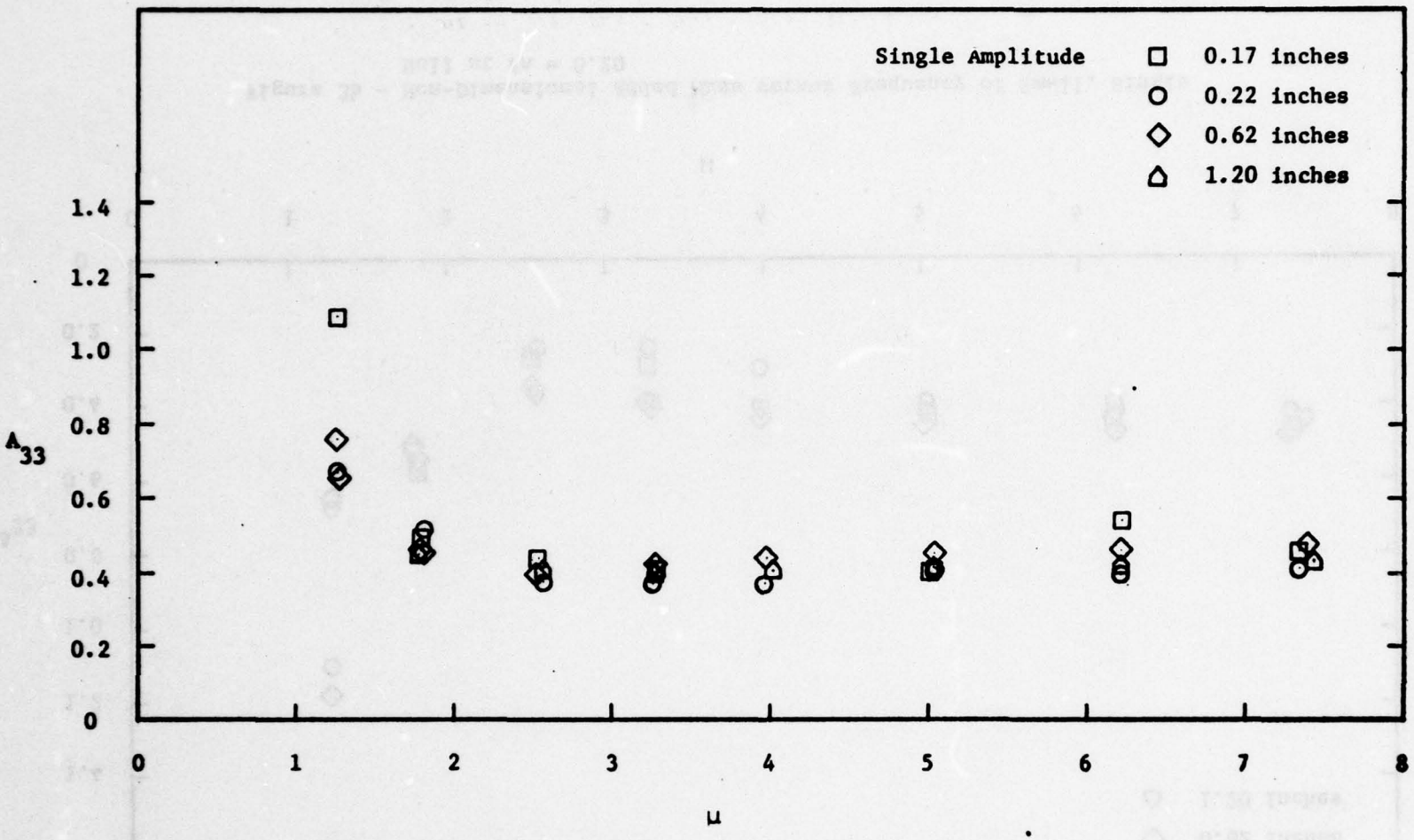

Figure 3c - Non-Dimensional Added Mass versus Frequency of Small, Single Hull at Fn = 0.40

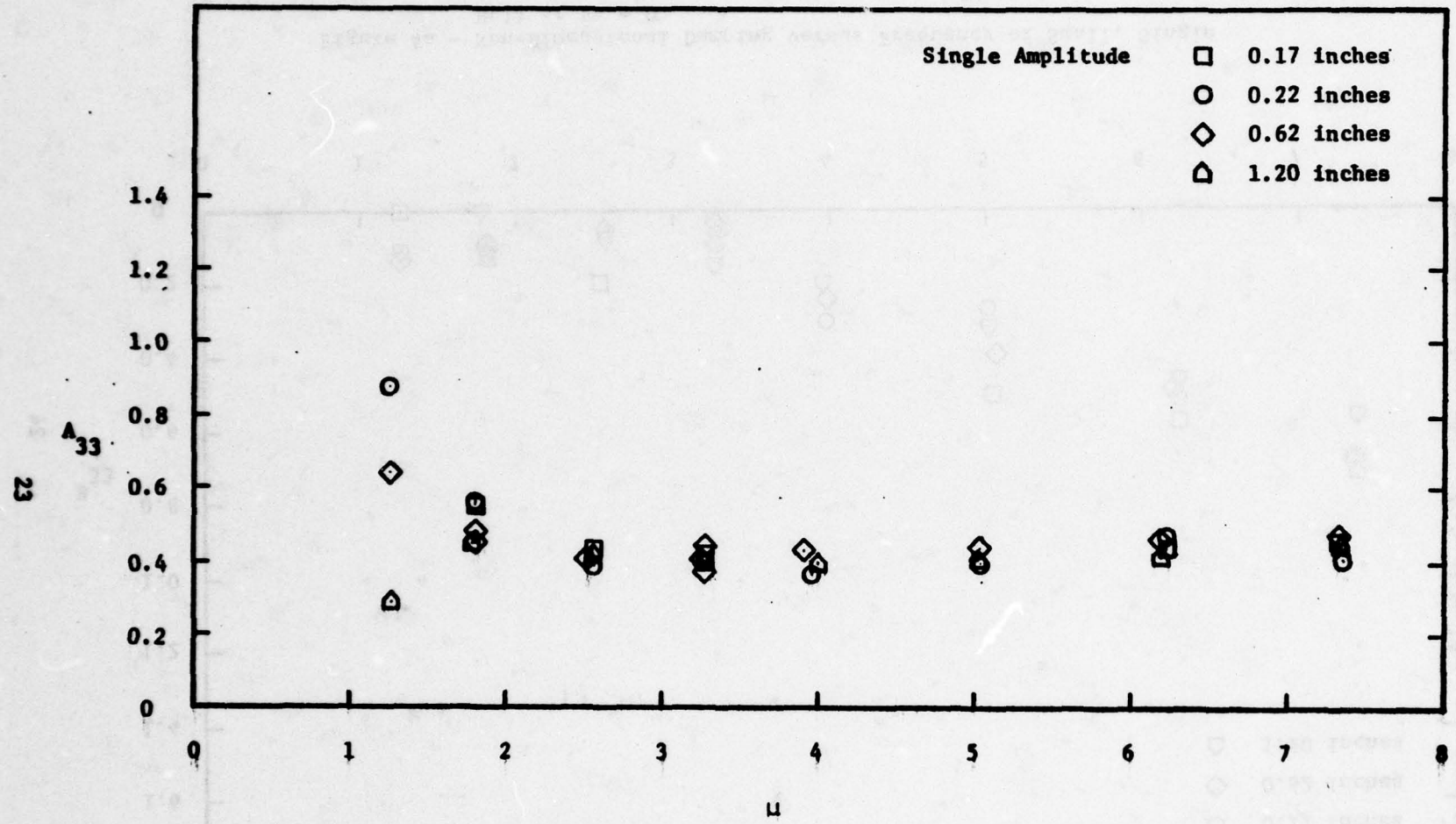

Figure 3d - Non-Dimensional Added Mass versus Frequency of Small, Single Hull at Fn = 0.60

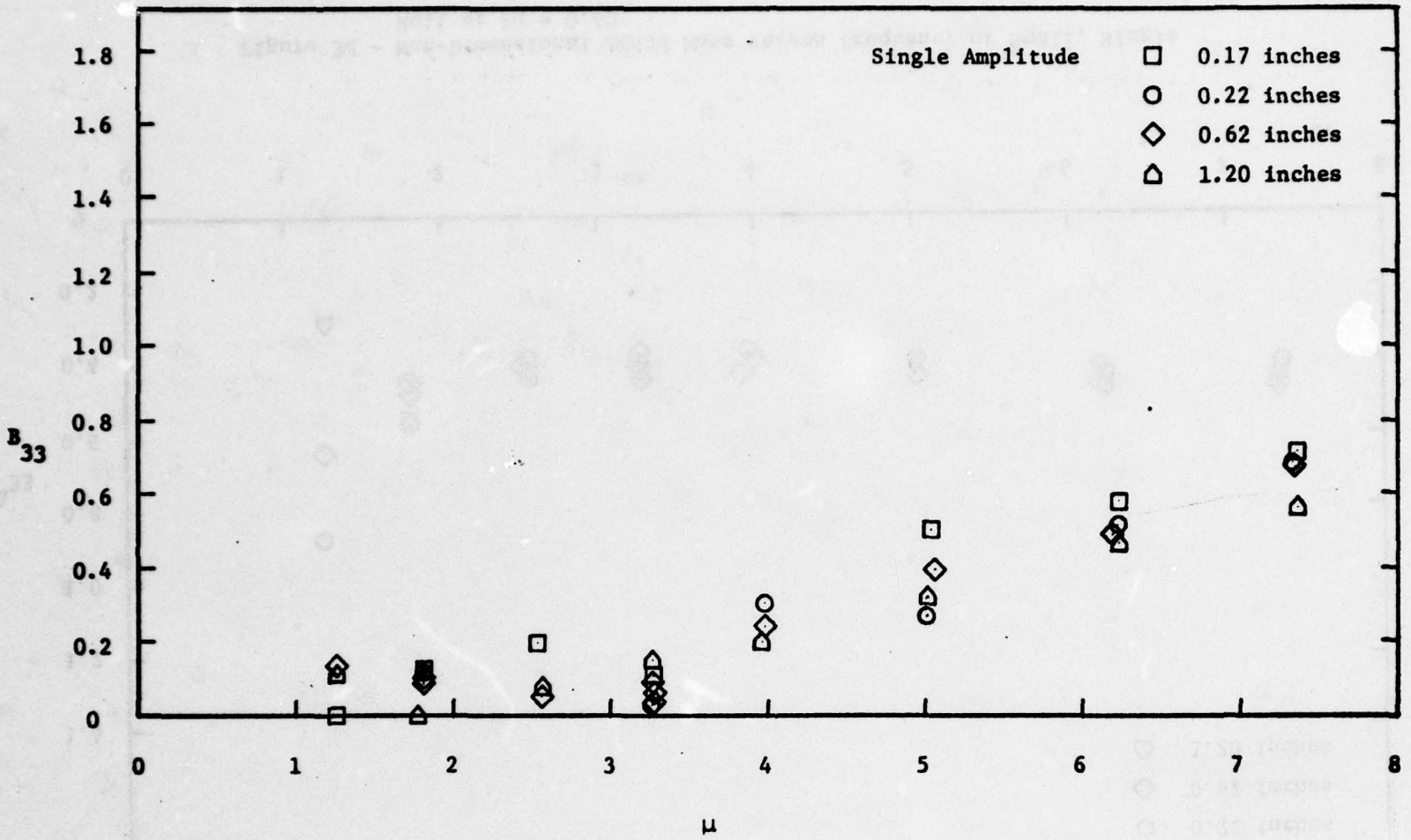

Figure 4a - Non-Dimensional Damping versus Frequency of Small, Single Hull at Fn = 0

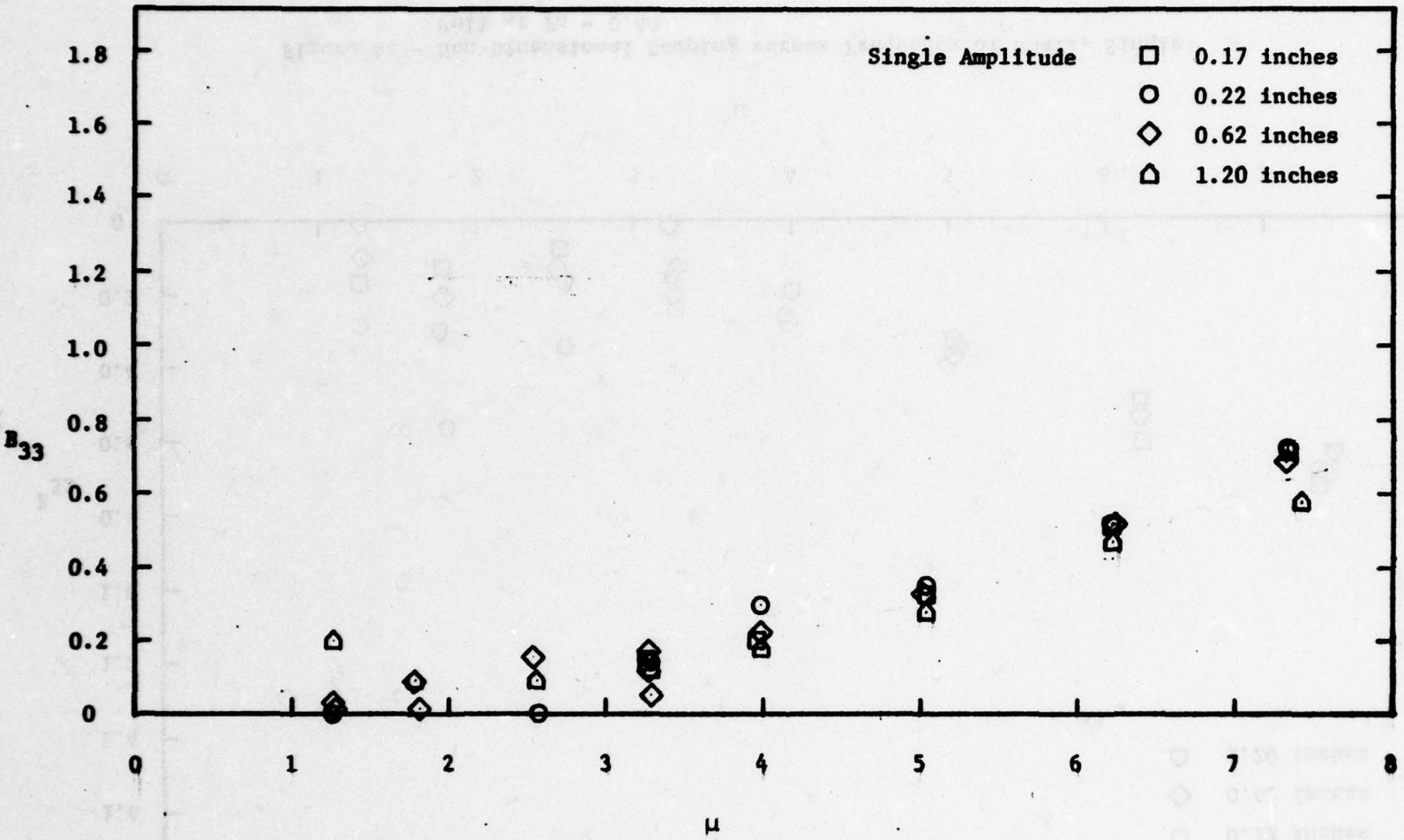

Figure 4b - Non-Dimensional Damping versus Frequency of Small, Single Hull at Fn = 0.20

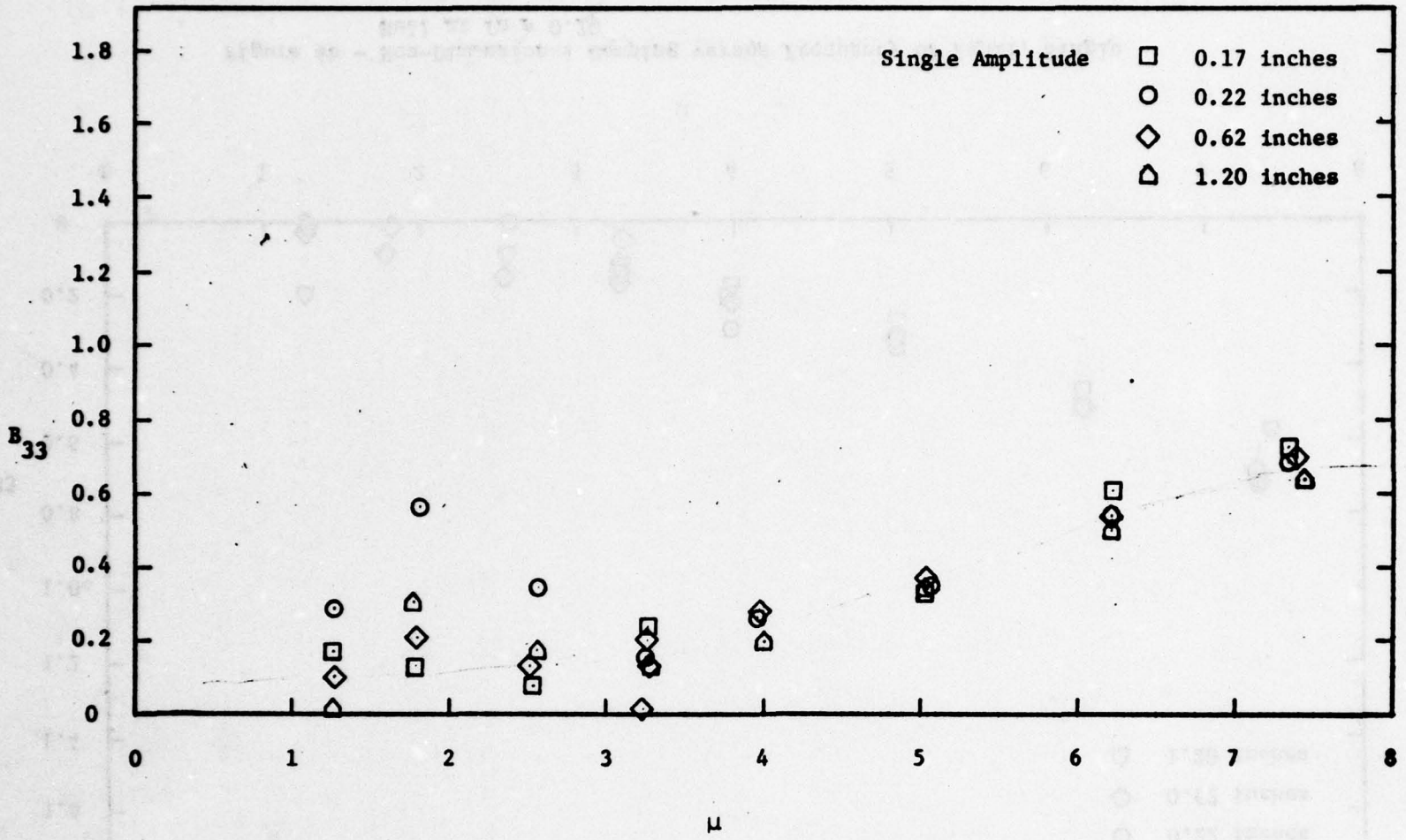

Figure 4c - Non-Dimensional Damping versus Frequency of Small, Single Hull at Fn = 0.40

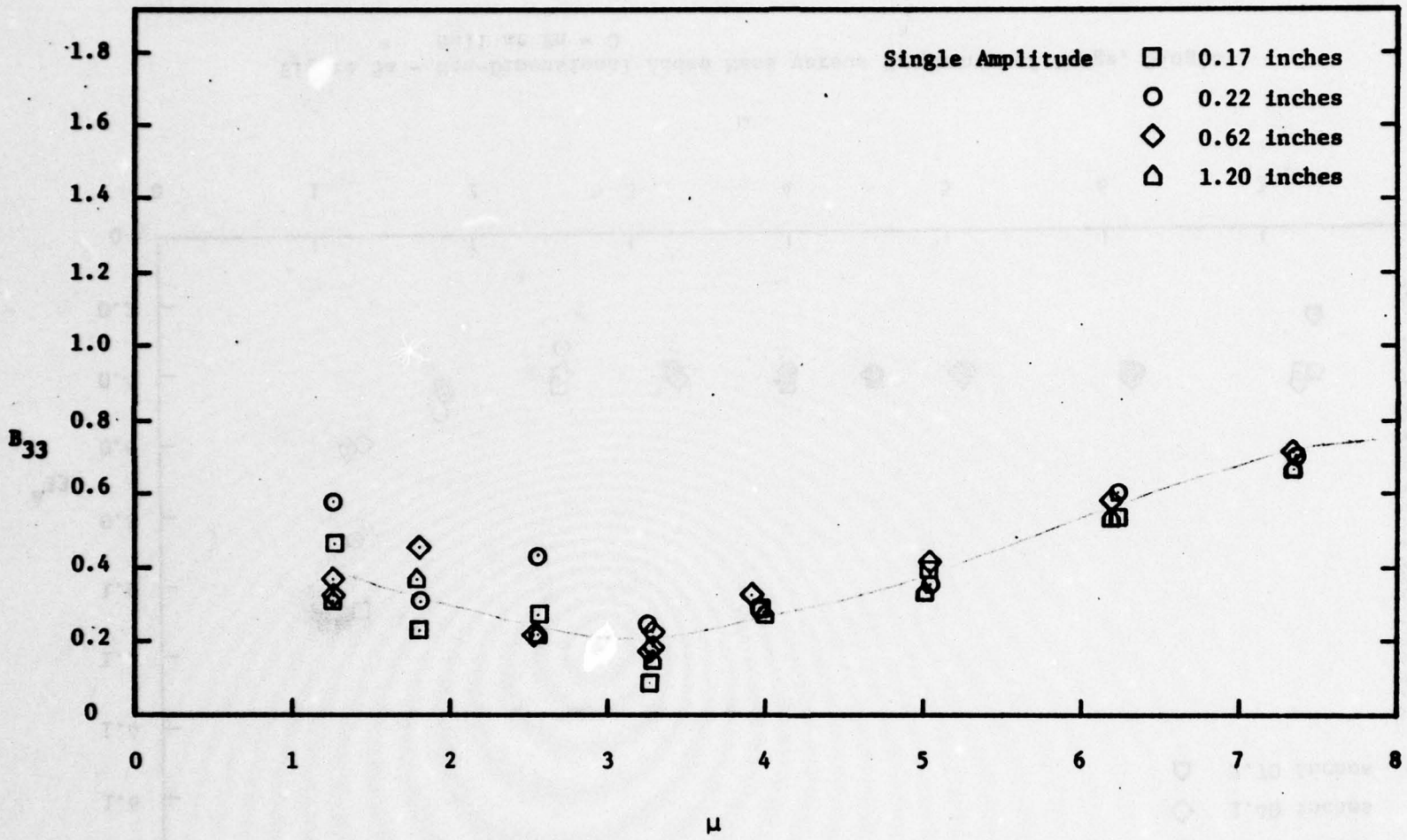

Figure 4d - Non-Dimensional Damping versus Frequency of Small, Single Hull at Fn = 0.60

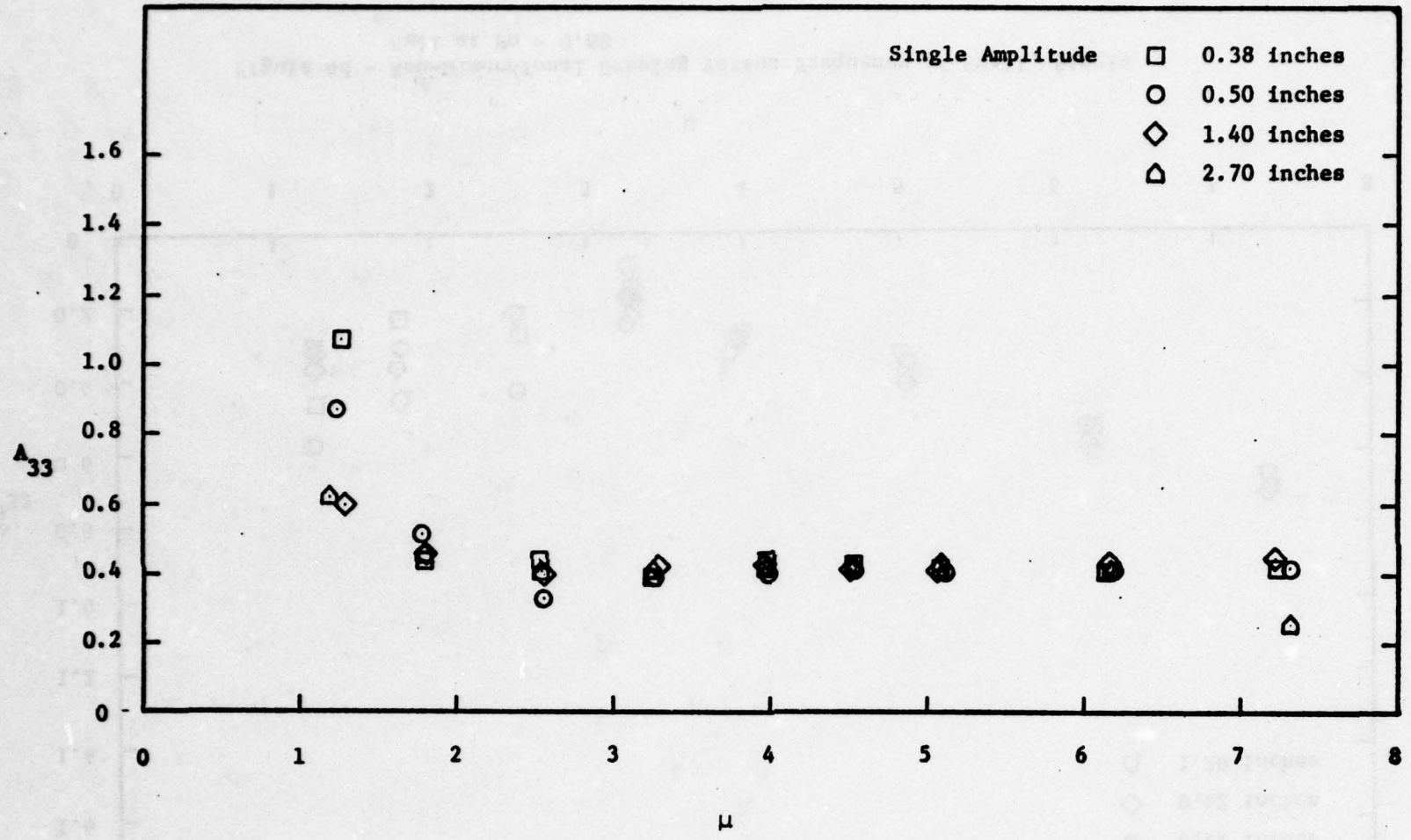

Figure 5a - Non-Dimensional Added Mass versus Frequency of Large, Single Hull at Fn = 0

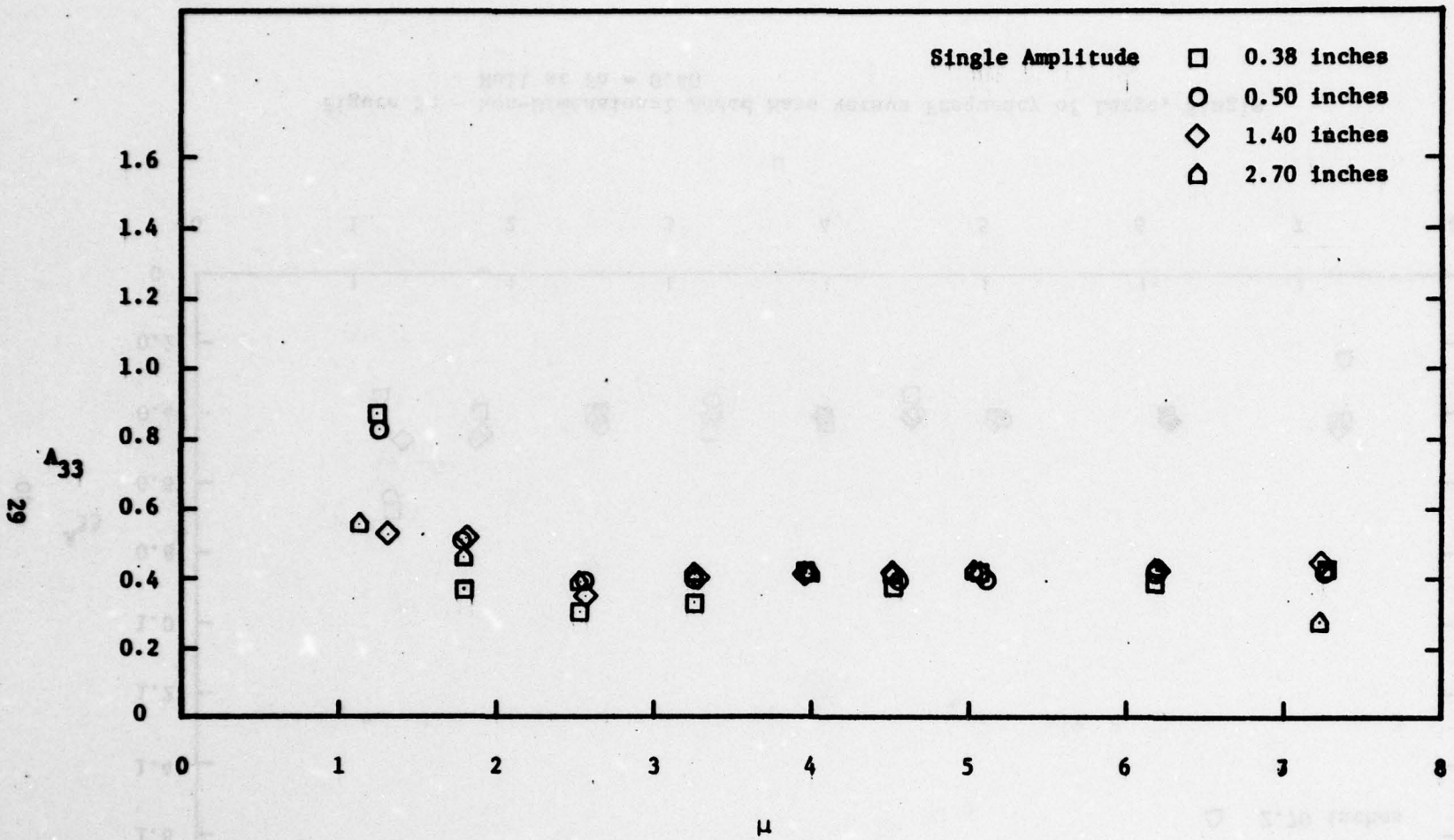

Figure 5b - Non-Dimensional Added Mass versus Frequency of Large, Single Hull at Fn = 0.20

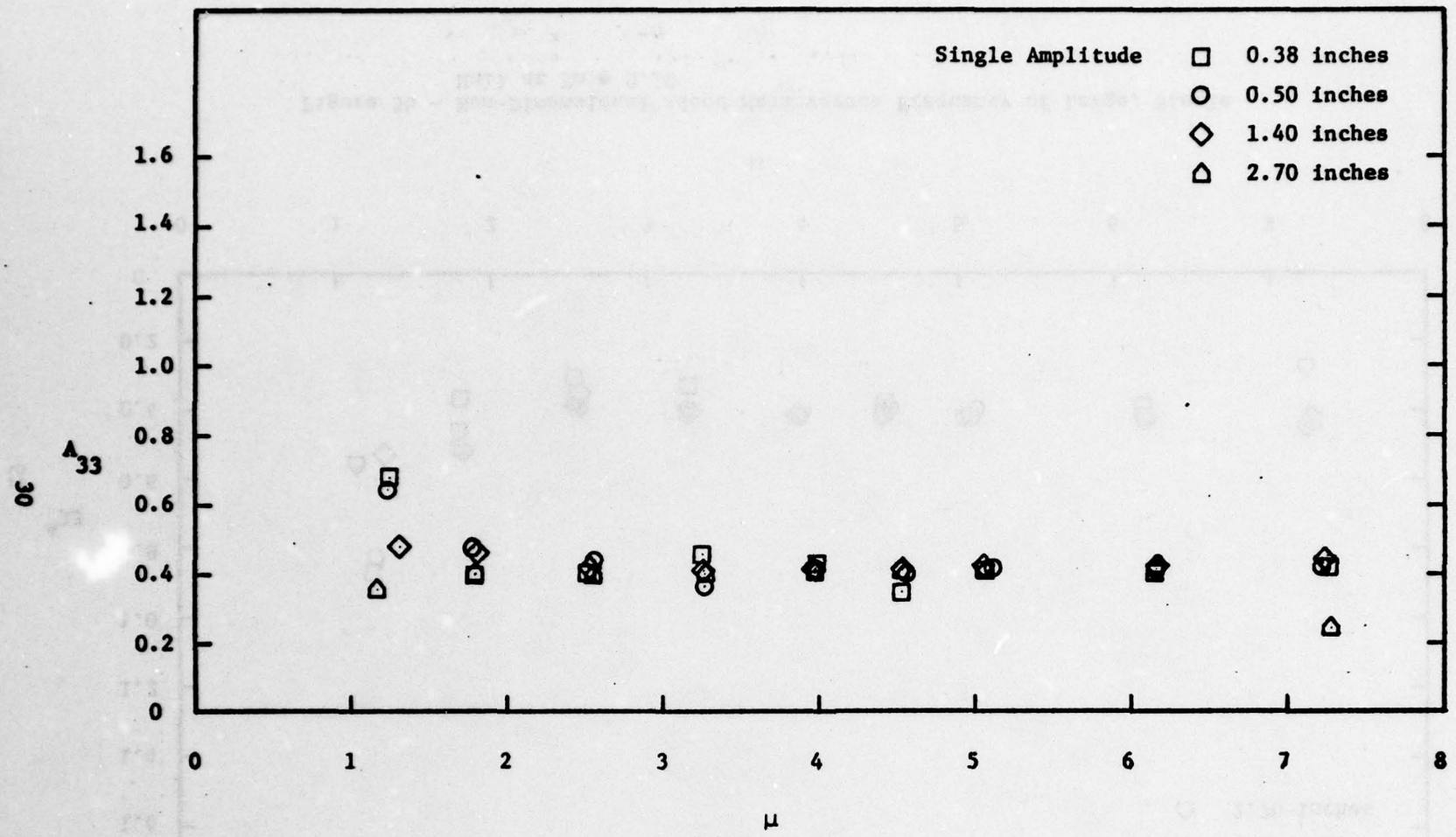

Figure 5c - Non-Dimensional Added Mass versus Frequency of Large, Single Hull at Fn = 0.40

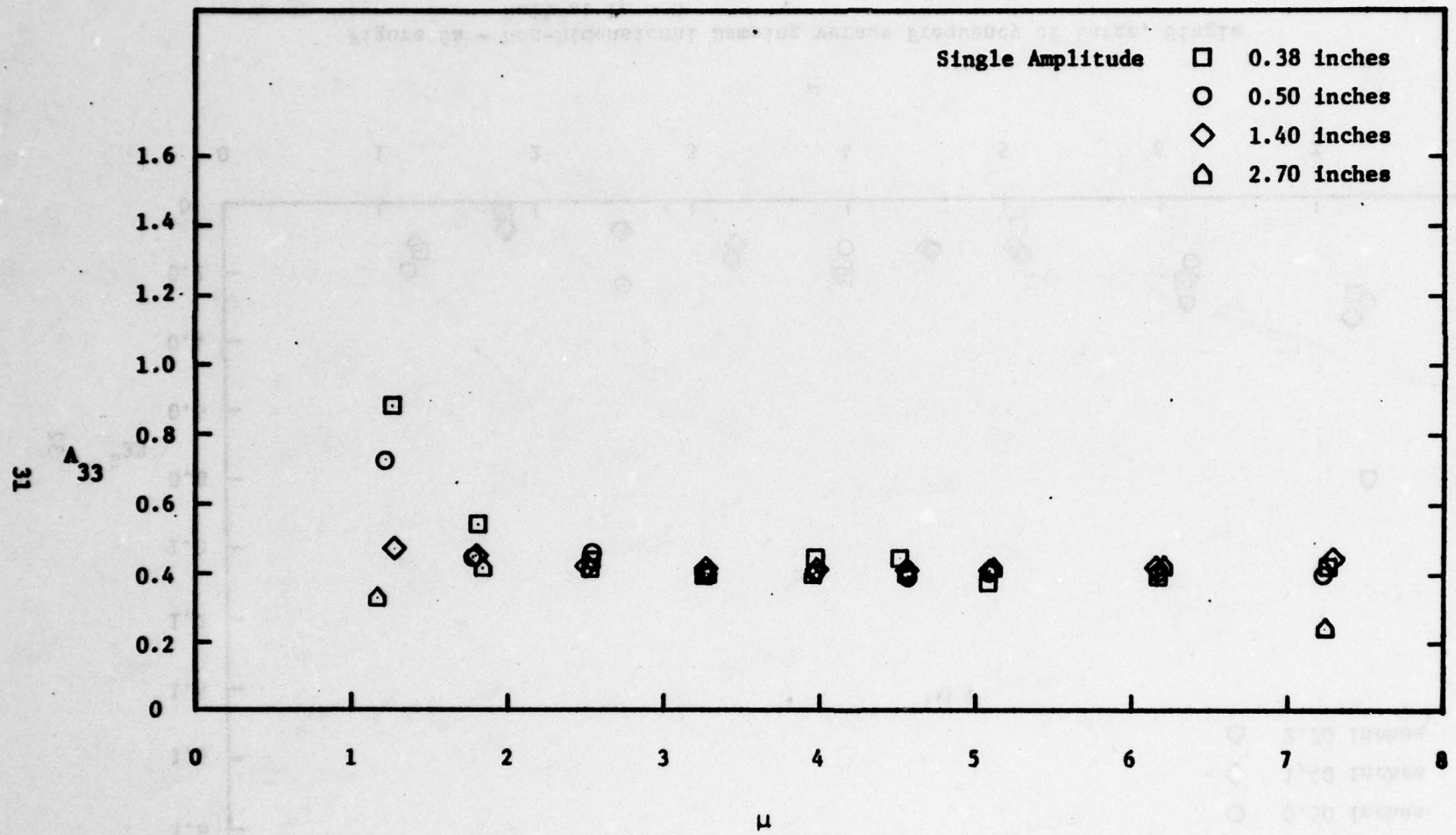

Figure 5d - Non-Dimensional Added Mass versus Frequency of Large, Single Hull at Fn = 0.60

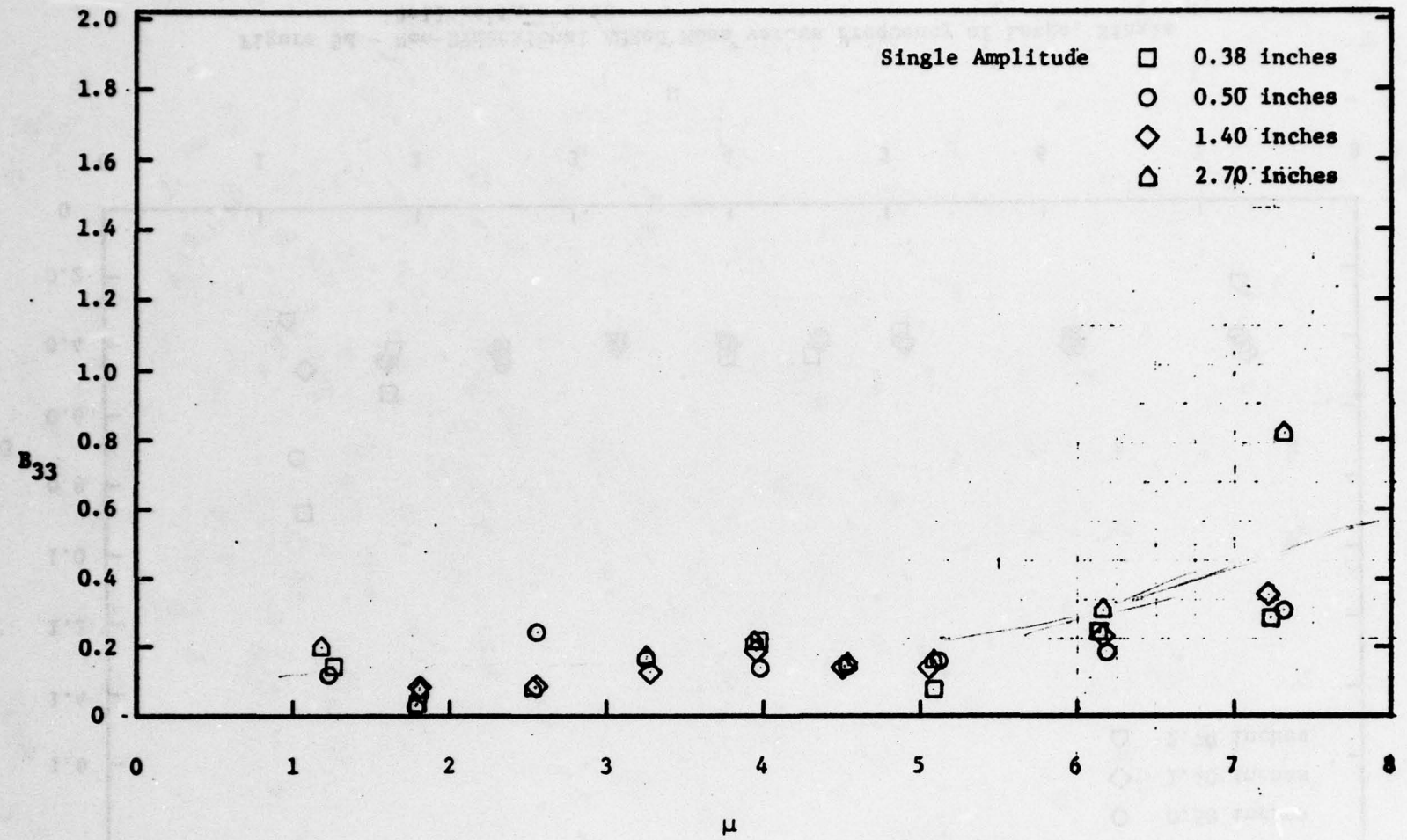

Figure 6a - Non-Dimensional Damping versus Frequency of Large, Single Hull at Fn = 0

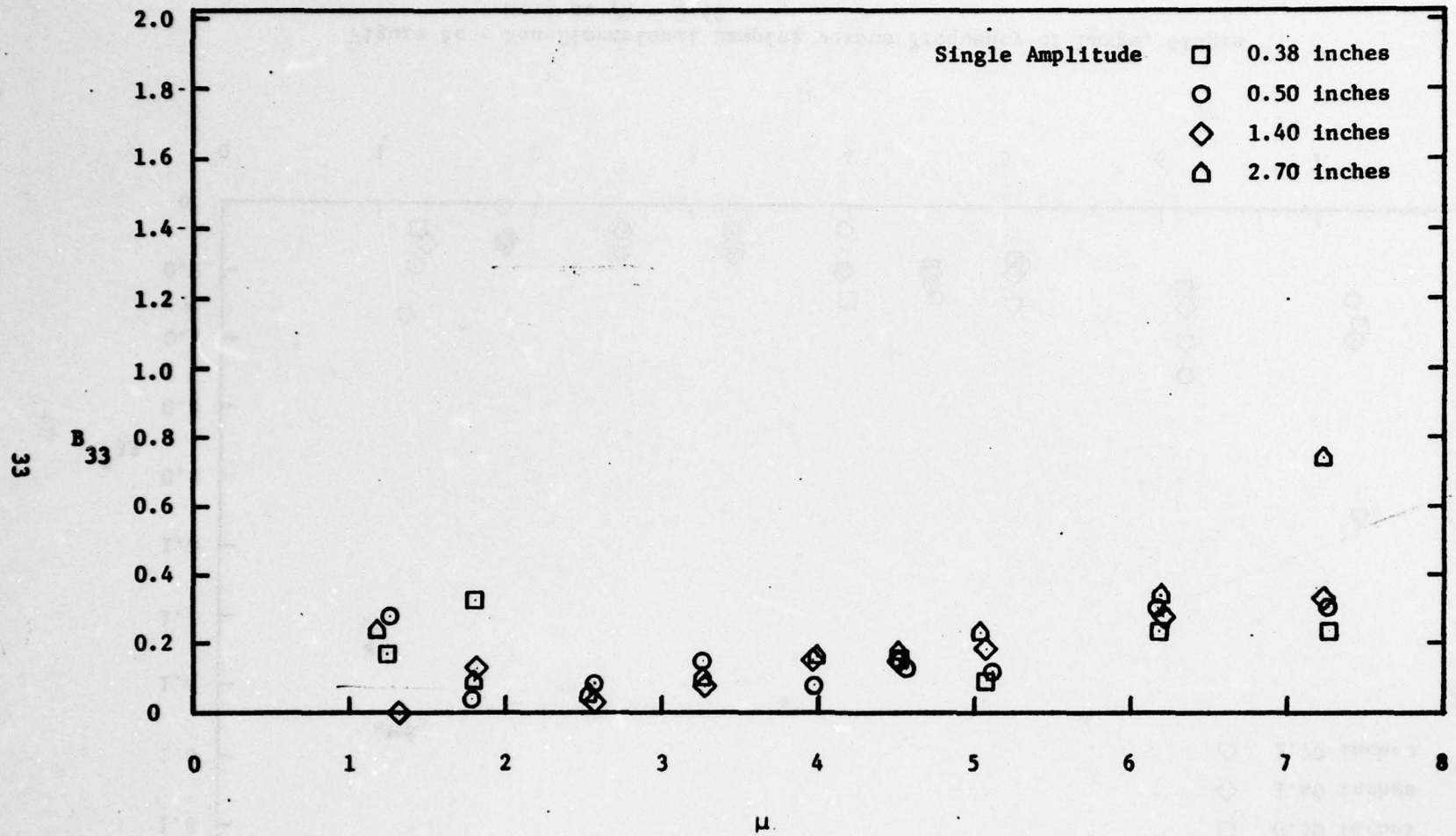

Figure 6b - Non-Dimensional Damping versus Frequency of Large, Single Hull at Fn = 0.20

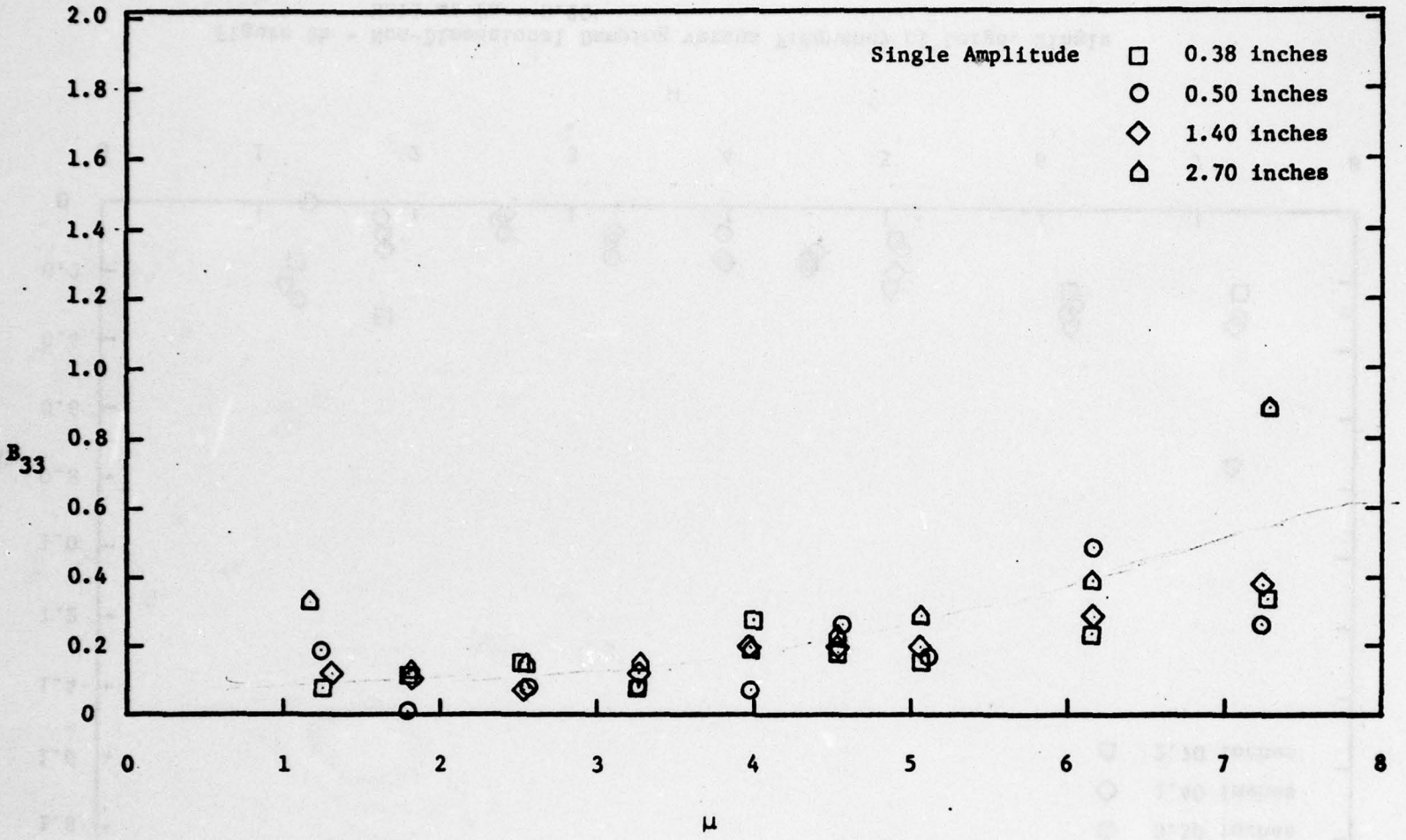

Figure 6c - Non-Dimensional Damping versus Frequency of Large, Single Hull at Fn = 0.40

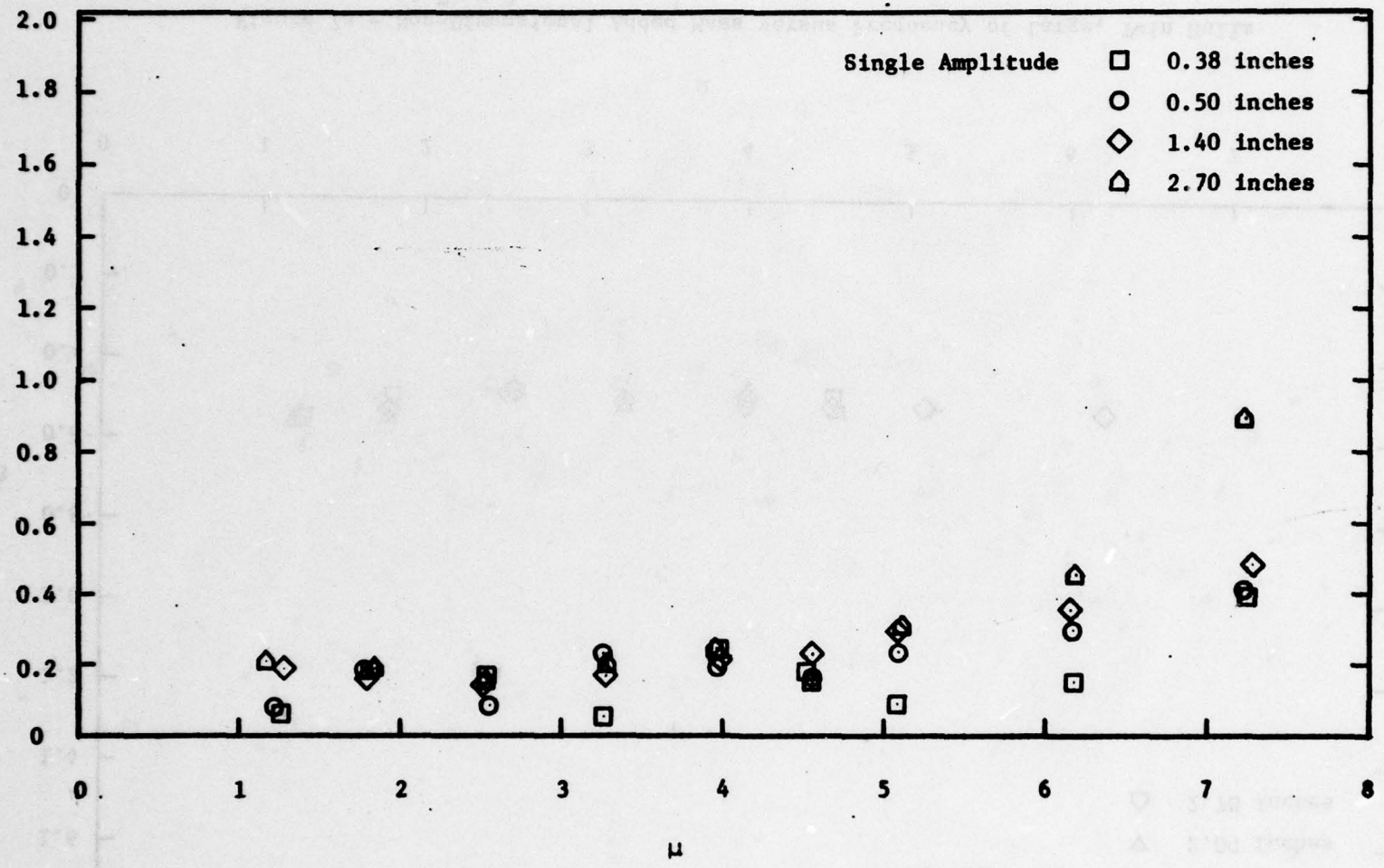

Figure 6d - Non-Dimensional Damping versus Frequency of Large, Single Hull at Fn = 0.60

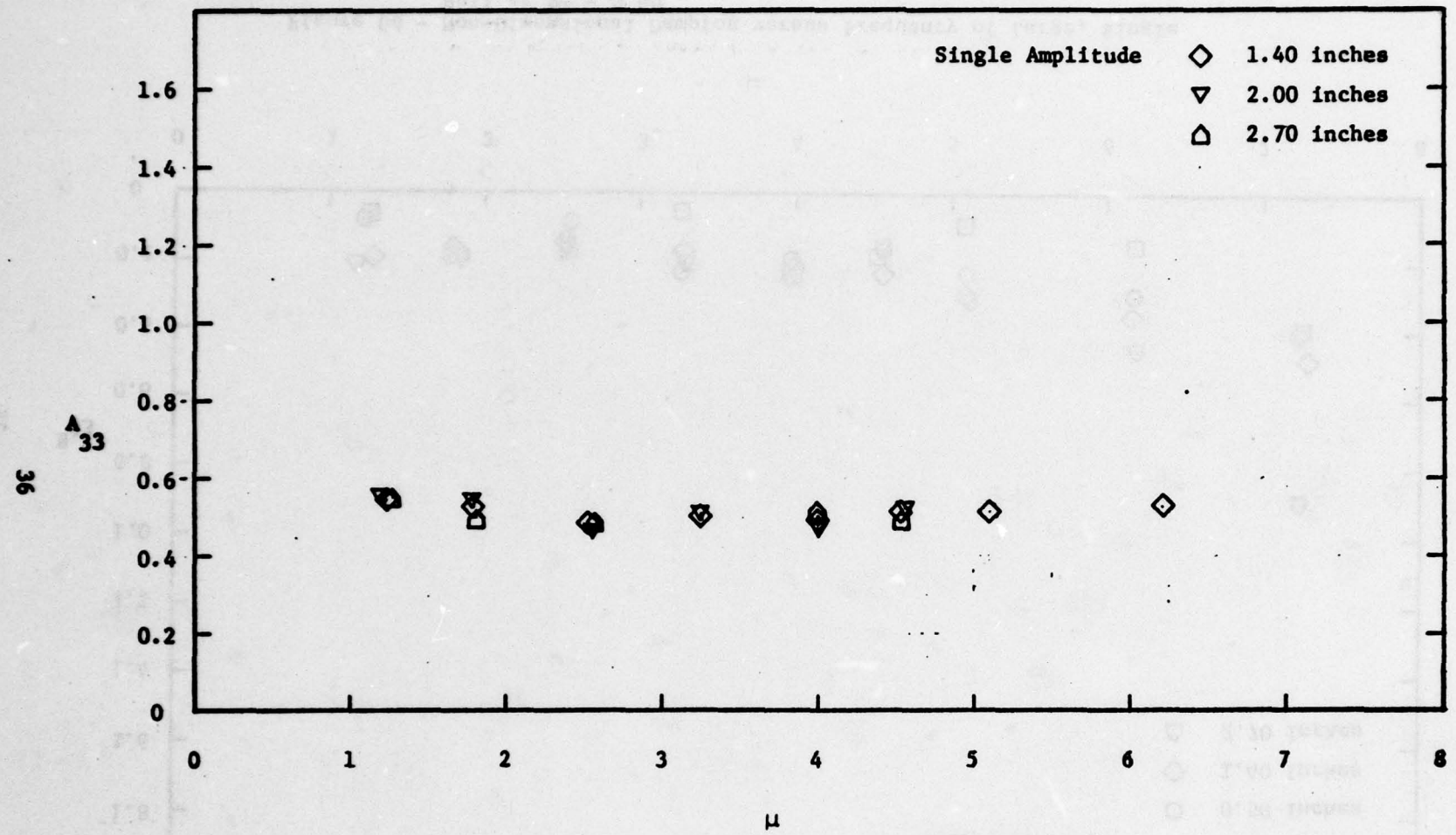

Figure 7a - Non-Dimensional Added Mass versus Frequency of Large, Twin Hulls at Fn = 0

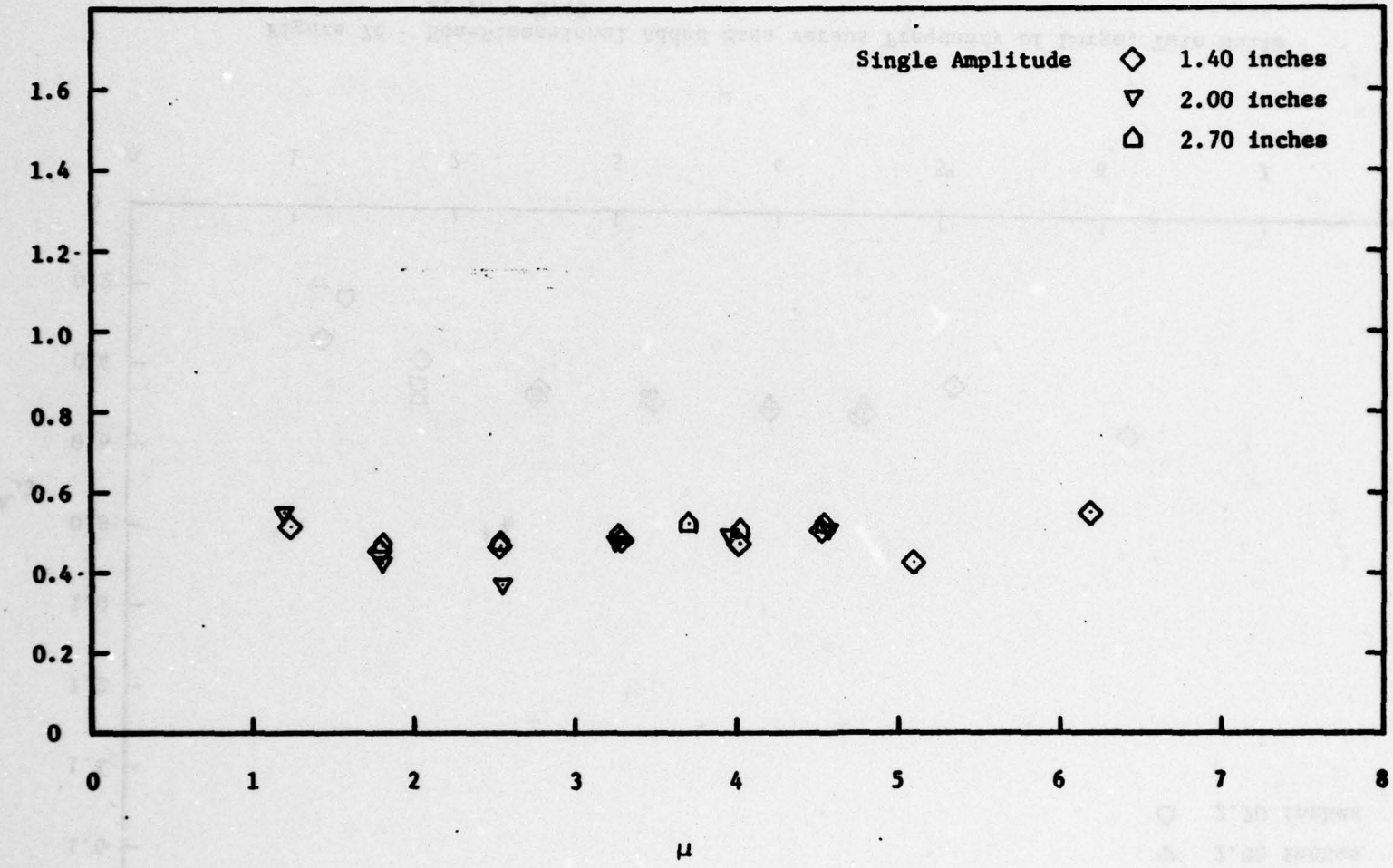

Figure 7b - Non-Dimensional Added Mass versus Frequency of Large, Twin Hulls at Fn = 0.20

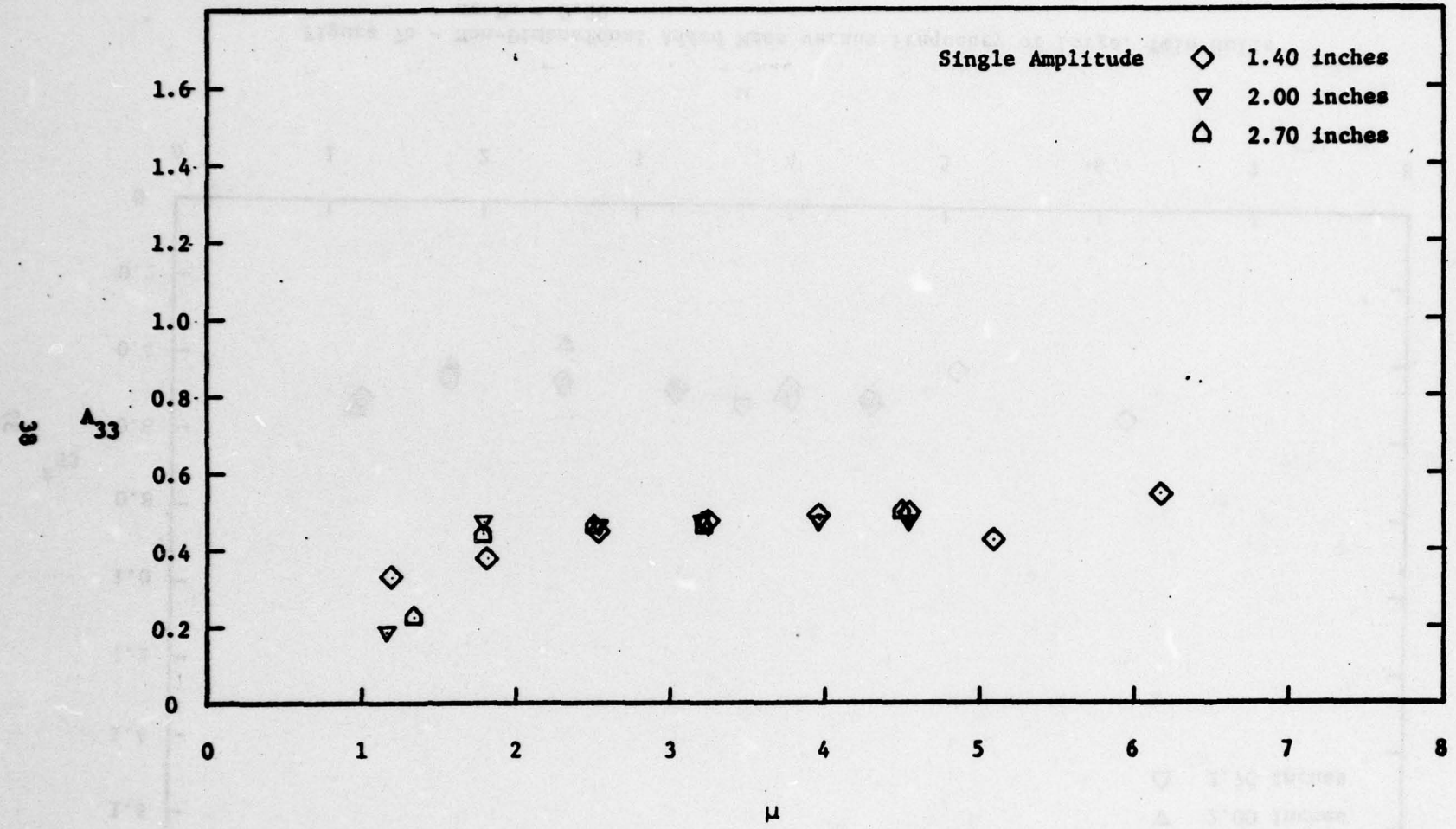

Figure 7c - Non-Dimensional Added Mass versus Frequency of Large, Twin Hulls at Fn = 0.40

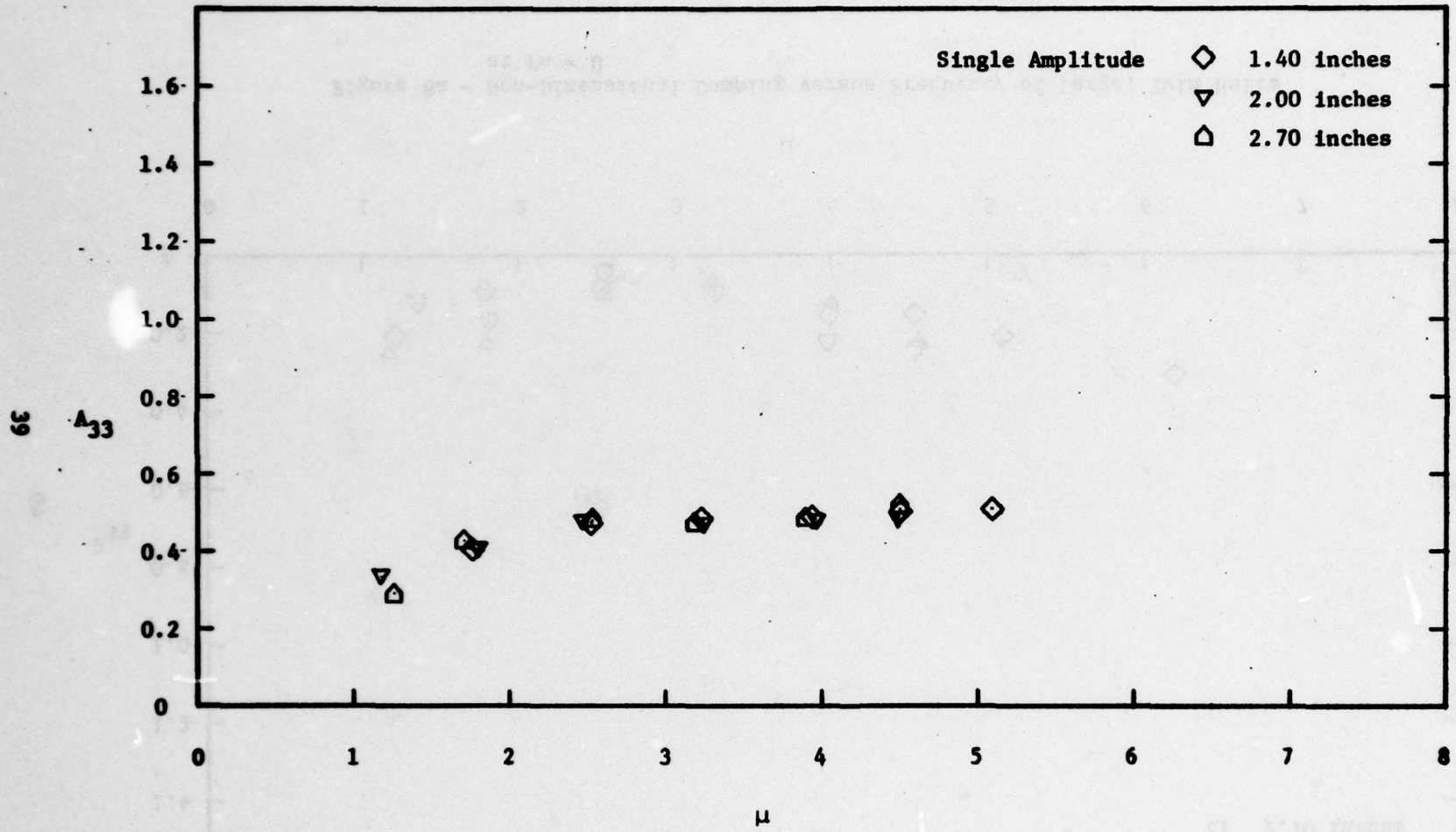

Figure 7d - Non-Dimensional Added Mass versus Frequency of Large, Twin Hulls at Fn = 0.60

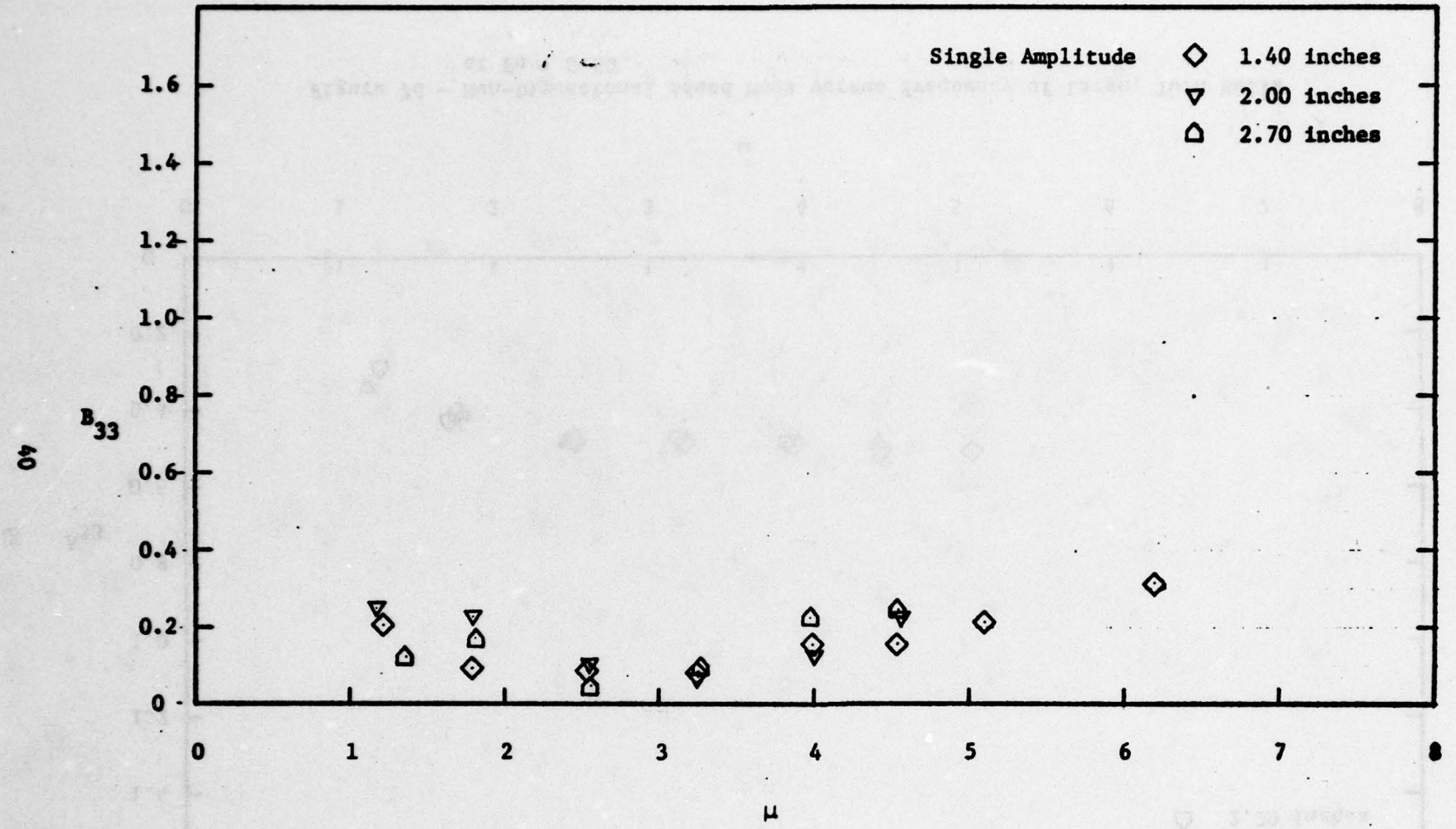

Figure 8a - Non-Dimensional Damping versus Frequency of Large, Twin Hulls at Fn = 0

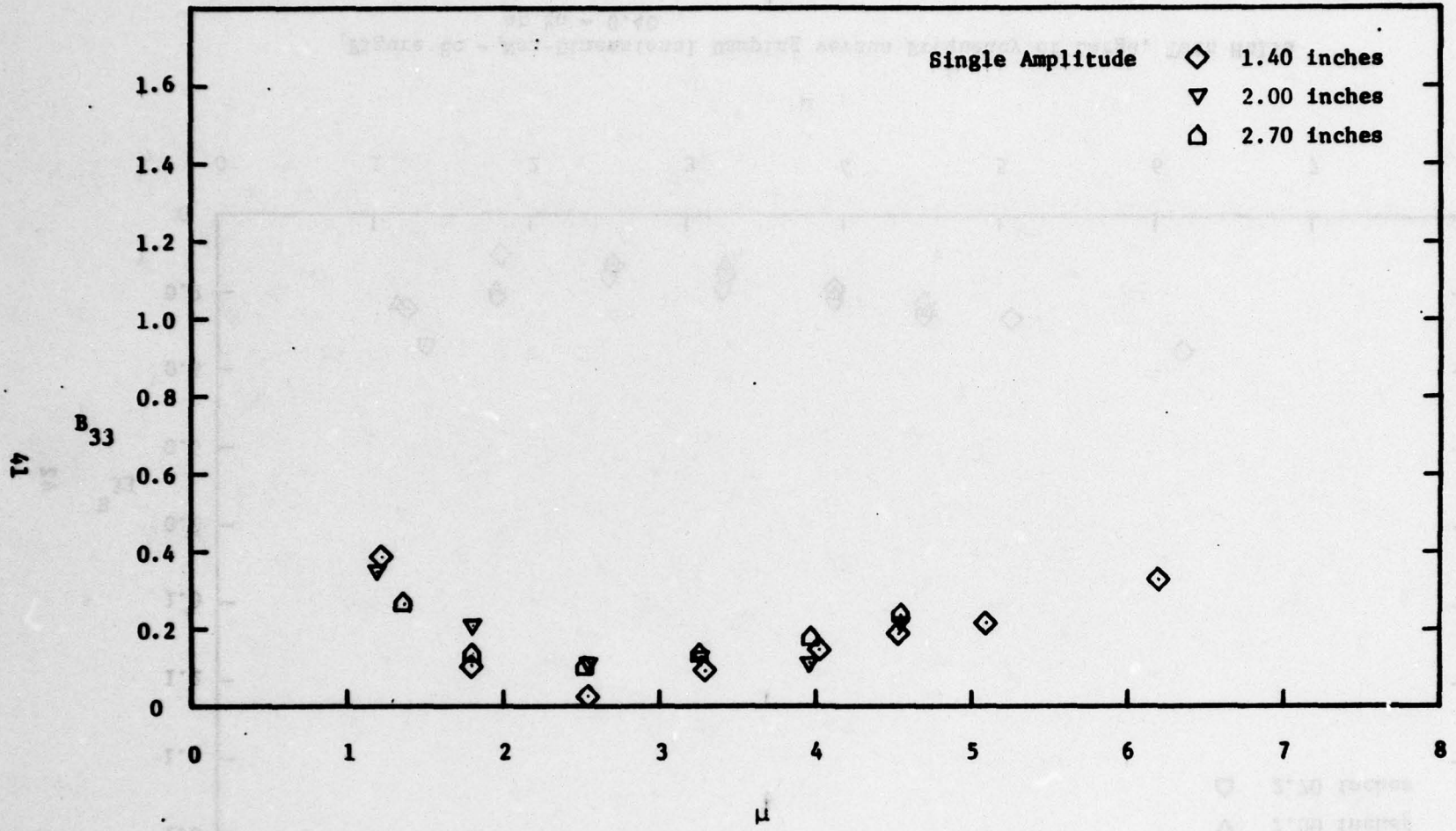

Figure 8b - Non-Dimensional Damping versus Frequency of Large, Twin Hulls at Fn = 0.20

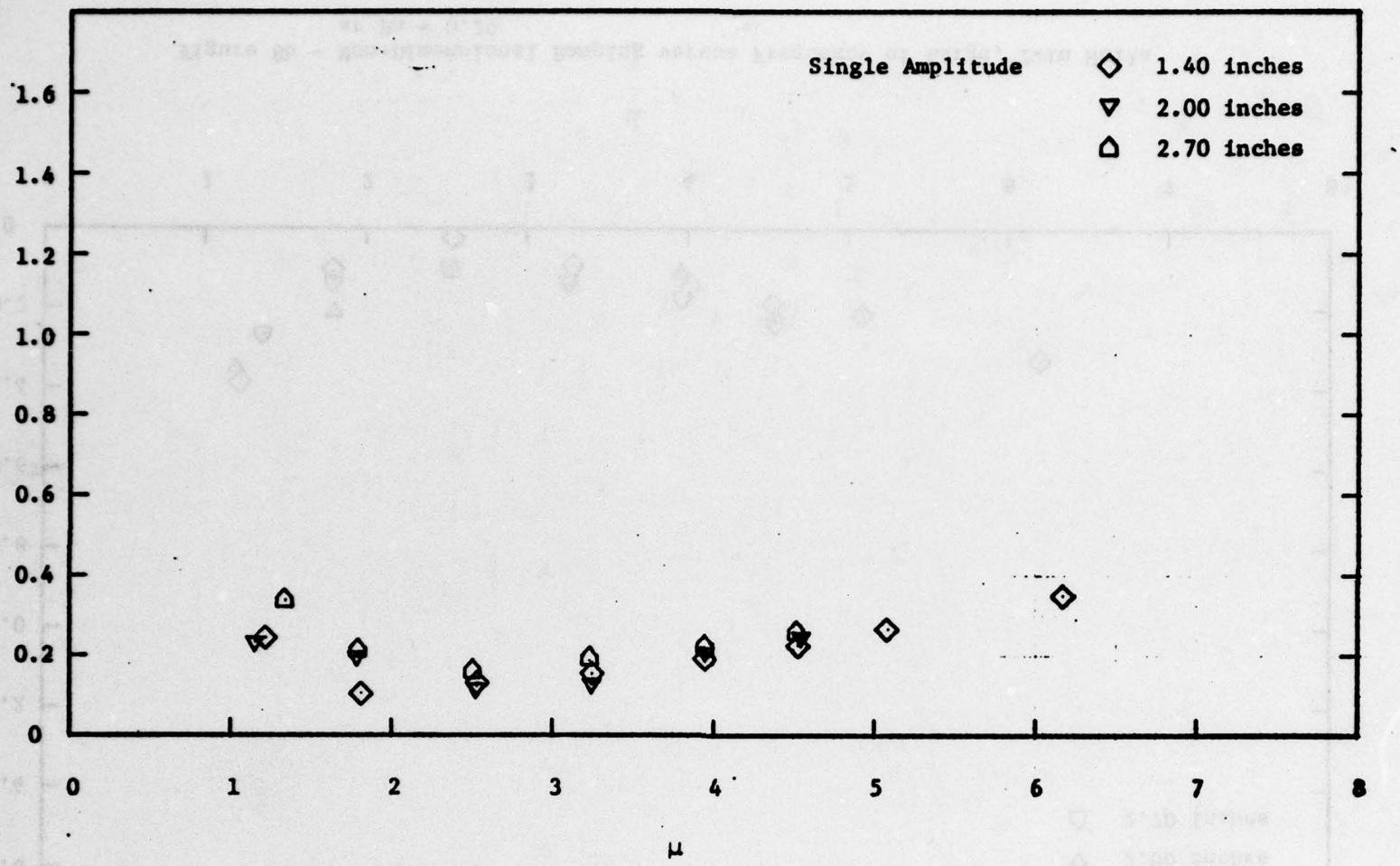

Figure 8c - Non-Dimensional Damping versus Frequency of Large, Twin Hulls at Fn = 0.40

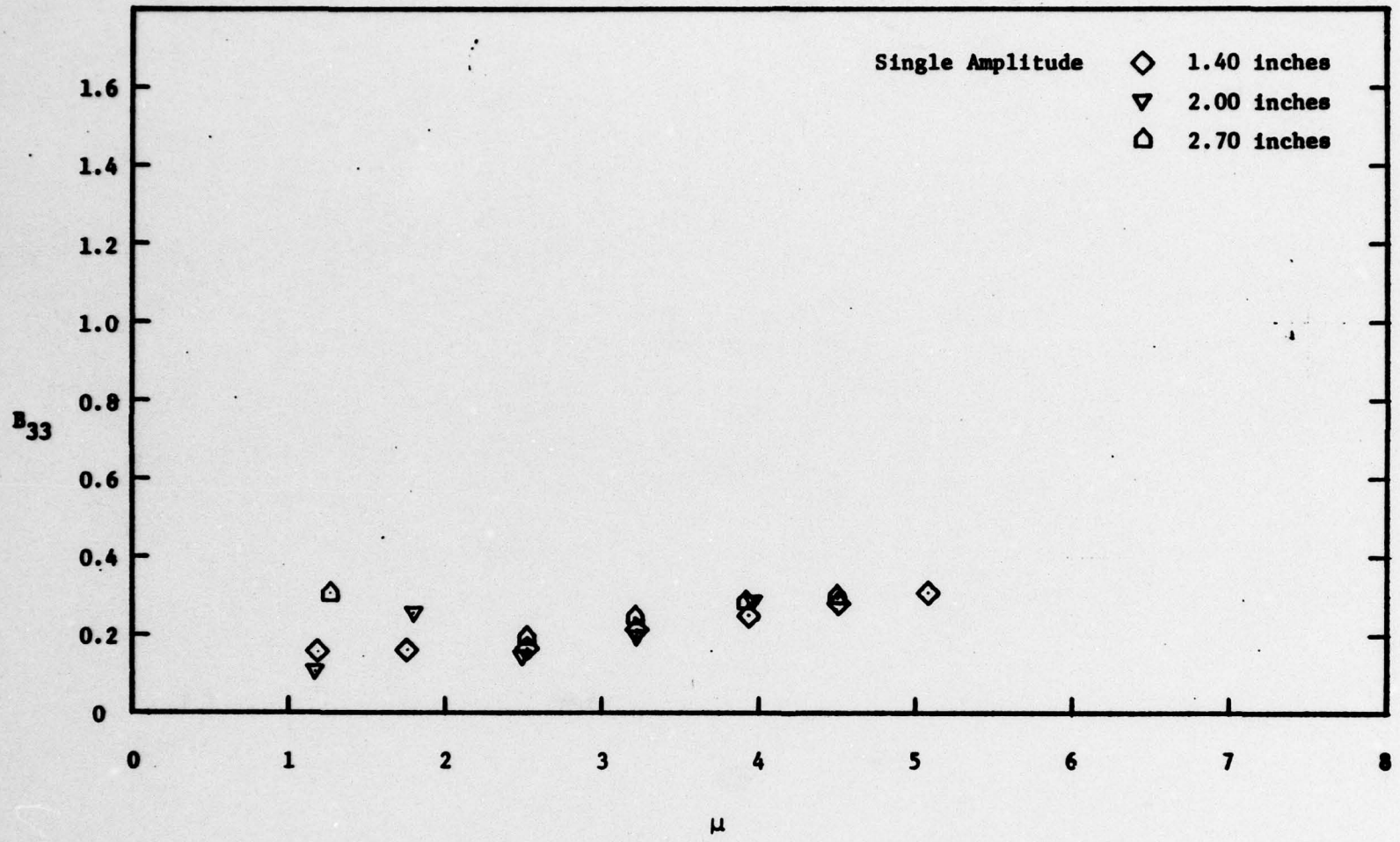

Figure 8d - Non-Dimensional Damping versus Frequency of Large, Twin Hulls at Fn = 0.60